Three-Dimensional Analysis on Thermal Stresses in A Perforated Disc Brake of Vehicle

by

Lee Jin Ming

Dissertation submitted in partial fulfillment of
the requirements for the
Bachelor of Engineering (Hons)
(Mechanical Engineering)

JAN 2010

Universiti Teknologi PETRONAS
Bandar Seri Iskandar
31750 Tronoh
Perak Darul Ridzuan

CERTIFICATION OF APPROVAL

Three-Dimensional Analysis on Thermal Stresses in A Perforated Disc Brake of Vehicle

by

Lee Jin Ming

A project dissertation submitted to the
Mechanical Engineering Programme
Universiti Teknologi PETRONAS
in partial fulfilment of the requirement for the
BACHELOR OF ENGINEERING (Hons)
(MECHANICAL ENGINEERING)

Approved by,

____

(Dr. Khairul Fuad)

UNIVERSITI TEKNOLOGI PETRONAS
TRONOH, PERAK
January 2010

CERTIFICATION OF ORIGINALITY

This is to certify that I am responsible for the work submitted in this project, that the original work is my own except as specified in the references and acknowledgements, and that the original work contained herein have not been undertaken or done by unspecified sources or persons.

____

LEE JIN MING

ABSTRACT

This report provides background information on small vehicle's perforated disc brake which is subjected to high frictional force during braking. This frictional action will consequently converts the car's kinetic energy into thermal energy in order to slow the car down. On the other hand, the thermal energy will be the source of thermal stresses in the perforated disc brake. The objectives of this project are to analyze and simulate three dimensional temperature and thermal stresses distribution within the perforated disc brake and to analyze the effect of having perforated holes by comparing the results with a non-perforated disc brake. The methodologies used in achieving these objectives are through numerical calculation and finite elements analysis by ANSYS. The temperature distributions obtain from the simulation show that maximum temperature produced by perforated and non perforated disc brakes is almost the same but perforated holes in perforated disc brake contributed to better temperature distribution within its cross section, giving better cooling effect. While for the thermal stress distribution, the generated Von Mises stress for perforated disc brake is lower than non perforated disc brake but high magnitude of Von Mises stress exists around the perforated holes. Furthermore, overall top surface Von Mises stress distribution shows that perforated disc brake has better stress distribution with extra lower stress region. Thus, it can be concluded through this project that perforated disc brake is better in increasing the performance of vehicle but the weighting are between high stress concentration at the perforated zones and better cooling ability as compared to conventional disc brake.

ACKNOWLEDGEMENT

First and foremost, the author would like to thanks Dr. Khairul Fuad, the respective project supervisor for his helps and guidance throughout the completion of this project. His keenness to share his knowledge and technical expertise in material science has directly contribution into the success in completing this project within the planned time. His constructive criticism and advices are very much appreciated.

The author would also like to express his gratitude to all research officers from Universiti Teknologi PETRONAS for sharing their thought and experiences on ANSYS simulation works.

Finally, great thanks to author's family and colleagues for their continuous support which kept the author well motivated.

TABLE OF CONTENTS

LIST OF FIGURES

LIST OF TABLES

CHAPTER 1
INTRODUCTION

1.1 BACKGROUND OF STUDY

Braking system in a vehicle is one of the most crucial components because apart from functioning as a mechanism to slow down the vehicle, it also affects the handling and safety performance of the vehicle. Two main components of the brake are the pad and the disc brake. The pad is essentially a piece of slim frictional material used to create a rubbing force against the disc brake surface in order to convert the vehicle's kinetic energy into thermal energy to slow and ultimately stops the vehicle. Furthermore, disc brake is being used to dissipate thermal heat produced during braking by providing sufficient surface for thermal convection and radiation. In sudden braking condition, high thermal heat is generated from the frictional force between the pad and disc brake. Thus, the materials used for both of these components have to be able to sustain high temperature without any failure. In the market, commonly used raw material for the disk brake is cast iron because it has high melting temperature of 1200 °C, easy to manufacture and relatively cheaper than other materials such as carbon disc.

As most of the generated thermal heat will be transferred to the disc brake, it will then functions as a small heat sink reservoir. In cases such as emergency braking, the disc brake might not be able to accumulate an infinite quantity of heat generated from continuous braking. Thus, the heat needs to be dissipated by having a good circulation of air which will be heated up when it is in contact with the hot surface of the disc and this keeps the disc brake from severe temperature that contributes to mechanical failure, or cracking. In order to increase the efficiency of heat dissipation from the disc brake, some disc brakes are vented by connecting "bridges" between two disc brakes to allow air flow in between them. Therefore, by having larger in contact surface with the air, heat is dissipated more effectively. Example of single disc and ventilated disc brake is shown in Figure 1 and Figure 2 below.

Figure 1.1: Single Plate Disc Brake

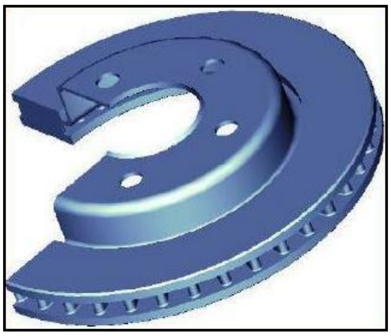

Figure 1.2: Ventilated Disc Brake

As for high performance vehicles such as racing car, conventional disc brake may not be sufficient enough in dissipating high generated heat, because of this perforated disc brake is being used instant of conventional disc brake. Perforated disc brake is also known as high performance or drilled disc brake as shown in Figure 1.3 below. Furthermore, perforated disc is commonly used in high performance vehicles due to its higher braking power especially during high speed travelling. But associated problem is that the brake pads will outgas and create boundary layer of gas between the pad and the disc if it is under use, hurting braking performance. Due to that, perforations are created to provide the gas someplace to escape. Although modern brake pads seldom suffer from out gassing problems, water residue may also build up after a vehicle passes through a puddle and impede braking performance.

However, perforated discs do have positive effect in wet condition because the perforated holes prevent a film of water building up between the disc and the pads as explained in Wikipedia.org [1]. Besides, the drilled holes also give more bite and allow air current (eddies) to blow through the disc brake to assist cooling and ventilating air so that more heat can be release by the disc surface onto the air as described by www.howstuffworks.com [2].

Figure 1.3: Perforated Disc Brake

1.2 PROBLEM STATEMENT

Light vehicle's disc brake experiences high temperature and forces especially during severe braking condition. Under such condition, the disc brake's surface temperature is much higher than its internal temperature due to the contact between the disc surface and the pad. This thermal shock due to the fast surge in temperature will contribute to the creation of thermal stress from uneven expansion of the disc brake between its surface volume and internal volume after a large number of cycles. These cycles of thermal stress arose from the braking may induce a number of unfavorable conditions such as material fatigue, surface cracking and permanent distortions. Ji-Hoon and In Lee [3] explained that frictional heating, thermal deformation and elastic contact in sliding contact systems affect the contact pressure and temperature on friction surfaces. These coupled thermal and mechanical behaviors can be unstable and lead to localized high temperature contact regions known as "hot spot" if the sliding speed is extremely high. These hot spots can cause material damage and ultimately thermal crack. Cracks are very much a big concern to the driver because they affect not only the braking performance of the vehicle but will also lead to braking failure.

For perforated disc brake, it poses a major setback in its application due to higher chance of cracking because the perforated holes are a source of stress cracks or zones with larger concentration of thermal stress under severe conditions as shown in Figure 1.4. According to www.carbibles.com [4], the drilling or perforation weakens the rotors and typically results in micro fractures to the rotor. The significant of this project is to carry out analysis on stresses arose due to high temperature or better known as thermal stresses and to examine how the perforation on the disc brake affects its performance. Furthermore, this project will verify the claim that the perforated holes are the main cause of cracking due to high concentration of stress around the perforated holes.

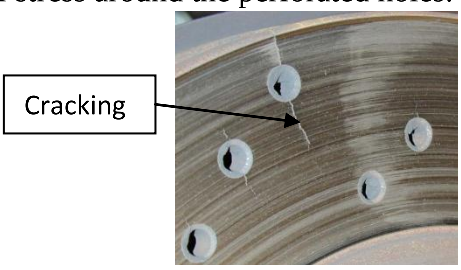

Figure 1.4: Cracking of Perforated Disc Brake

1.3 OBJECTIVES

The objectives of this project are stated as below:

1. To analyze and simulate three dimensional temperature and thermal stress distribution in a perforated brake disc of small vehicle during braking using ANSYS.
2. To compare the temperature and thermal stress distribution between perforated and non-perforated brake disc.

1.4 SCOPE OF STUDY

In this project, a pair of perforated and non-perforated disc brakes and brake pads will be considered for further analysis as per stated in the objectives. It involves the contact between the brake pad and disc brake to create sufficient frictional force in order to slow the wheel. Thermal stresses arise due to this high frictional force and temperature. So it is important to perform the analysis on thermal stress as stress will ultimately leads to thermal cracking of the disc brake and stress analysis is one of the crucial aspects in designing sliding contact systems.

In the analysis, the pressure distribution imposed by the brake pad onto the disc brake is assumed to be uniform throughout the contact area for the ease of analysis and also it is assumed that the frictional heat flux at the contact area is constant along the surface. Besides, this project involved a lot of applications and knowledge from various mechanical engineering fields of thermodynamic, finite element analysis, computer aided design and engineering and stress analysis.

CHAPTER 2
LITERATURE REVIEW

There are three types of mechanical stresses subjected by the disc brake as shown in Figure 2.1. The first one is the traction force created by the centrifugal effect due to the rotational of the disc brake when the wheel is rotating and no braking force is applied to the disc. During braking operation, there are another two additional forces experienced by the disc brake. Firstly, compression force is created as the result of the force exerted by the brake pad pressing perpendicular onto the surface of the disc to slow it down. Secondly, the braking action due to the rubbing of the brake pad against the surface of the disc brake is translated into frictional or traction force on the disc surface which acts in the opposite direction of the disc rotation. It is due to this frictional force that heat is generated, increases the temperature of the disc brake and contributes to the rise of thermal stresses. Thermal stresses will exist in a material whenever temperature gradients are present within it.

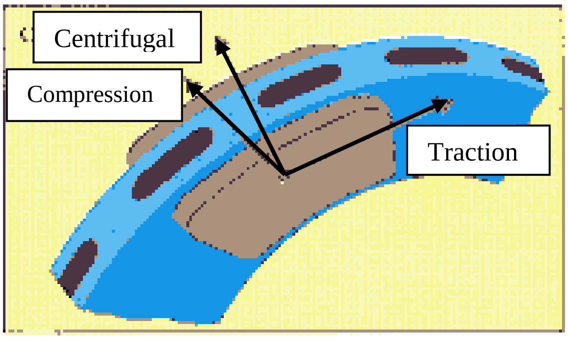

Figure 2.1: Mechanical Stresses on Disc Brake

The different in temperatures produces different expansions and subject materials to internal stress. Mohd Adam (2009, p.5) [5] points out that the major sources of thermal stress are restrained thermal expansion or contraction and temperature gradient established during heating or cooling process. The thermal stress which developed if a structure or material is completely constrained is the product of the coefficient of linear expansion (α), the temperature change (ΔT) and Young's modulus (E) for the material where the relationship is given by:

$$\sigma = \alpha\,(\Delta\ T)\,E \qquad (2\text{-}1)$$

As referring to Robert W. Soutas-Little (1999, p. 78-80) [6], the effect of temperature change can be introduced into the theory of elasticity by examining the strain energy function, W which is based on Hooke's Law. For a hyperelastic material, a strain energy function W is assumed to exist, with property of:

$$\sigma_{ij} = \frac{\delta W}{\delta \in_{ij}} \qquad (2\text{-}2)$$

The existence of this function can be shown to place symmetry constraints on the constants involved in the generalized Hooke's Law.

$$\sigma_{ij} = C_{ijrs} \in_{rs} \qquad (2\text{-}3)$$

If the material obeys Hooke's law, the stain energy function can be written as:

$$W= \frac{1}{2} C_{ijkl} \in_{ij} \in_{kl} \qquad (2\text{-}4)$$

In accounting the effect of temperature change in the theory of elasticity, W is assumed to be in the form of a power series expansion in strain, giving:

$$W = C_o + C'_{ij} \in_{ij} + \frac{1}{2} C_{ijkl} \in_{ij} \in_{kl} + \ldots. \qquad (2\text{-}5)$$

The stress tensor may be related to the strain tensor by the relationship of:

$$\sigma_{ij} = \frac{\delta W}{\delta \in_{ij}} = C'_{ij} + C_{ijkl} \in_{kl} \qquad (2\text{-}6)$$

The second term leads to the generalized Hooke's law and the first term implies that stresses may present in a body which is in a state of zero strain where such stresses may arise if a liner expansion occurs due to temperature changes. The simplest assumption is to assume that C'_{ij} is linearly proportional to the temperature change $(T\text{-}T_o)$ and equal in all directions for isotropic material:

$$C'_{ij} = -\alpha\,(3\lambda+2\mu)\,(T\text{-}T_o)\delta_{ij} \qquad (2\text{-}7)$$

where α is coefficient of linear thermal expansion.

The stress-strain relation then becomes:

$$\sigma_{ij} = \lambda\,\delta_{ij} \in_{kk} + 2\mu \in_{ij} - \alpha\,(3\lambda+2\mu)\,(T\text{-}T_o)\delta_{ij} \qquad (2\text{-}8)$$

Above equation is known as the Duhamel – Neumann generalization of Hooke's law. The thermal strain equation can be obtained by adding a thermal expansion term to the strain equation:

$$\epsilon_{ij} = \frac{1}{2\mu}\left[\sigma_{ij} - \frac{\lambda}{3\lambda+2\mu}\sigma_{kk}\,\delta_{ij}\right] + \alpha\,\delta_{ij}\,(T-T_o) \qquad (2\text{-}9)$$

According to D.J. Kim, Y.M. Lee, J.S. Park and C.S. Seok (2008, p. 456-459) [7], thermal stresses are generated by the cyclic frictional heat and thermal fatigue cracks are generated by the thermal stress on a frictional plate. Therefore, in order to secure the braking stability and to improve the fatigue life of a disk brake, it is necessary to research the thermal stress on a disk brake. Furthermore, J.H. Choi and I. Lee (2004, p. 47–58) [3] mentioned that thermal stresses due to high temperatures may induce a number of unfavorable conditions such as surface cracks and permanent distortions. Frictional heating, thermal deformation and elastic contact in sliding contact systems affect the contact pressure and temperature on the friction surfaces. Based on journey by Thomas J. Mackin and group (2002, p.63-76) [8], thermal cracking in disc brake rotors is a low cycle thermo-mechanical fatigue problem and there are three ways to eliminate thermal cracking in brake rotors: (1) increase the yield and fatigue strength of the rotor material; (2) decrease the braking temperatures; and/or (3) re-design the hub–rotor unit to eliminate constraint stresses.

Although the perforated holes are initially designed to provide better grip to the disc brake and increases its frictional property, the holes themselves might appear to be the localized high temperature contact area. This area will experiences higher metal fatigue and initiates the thermal crack. Further analysis by using finite element method will be used to compute the temperature and thermal stresses distribution on the surface of the perforated disc brake. Finite element method is known as a powerful tool for many engineering simulations was widely used to compute the distributions of thermal elastic, elastic–plastic, residual stresses and thermal stresses and finite element method is a numerical technique for finding approximate solutions of partial differential equations as well as of integral equations as described in Wikipedia.com [9]. For this reason, ANSYS, a general purpose code, was preferred in the analysis of the thermal stress problem. Moreover, finite element solution to be carried out by ANSYS will divides the modeled three dimension disc brake volume into smaller elements and nodes by mesh generation process to evaluate the thermal stress distribution within the disc brake.

CHAPTER 3
METHODOLOGY

3.1 METHODOLOGY

The three dimensional model of disc brake will be modeled by using computer design software from CATIA. This model can be further analyzed by performing finite element analysis method with the help of engineering software ANSYS capable of running the simulation and analysis for required conditions. Firstly, calculated heat flux generation will be applied to the disc brake model with the help of ANSYS to investigate the resulting temperature distribution. Next, the acquired heat distribution will be use as the input to further investigating the corresponding thermal stresses on the disc brake. The methodology used is presented in Figure 3.1 below. Please refer to Appendix G for project's Gantt Charts.

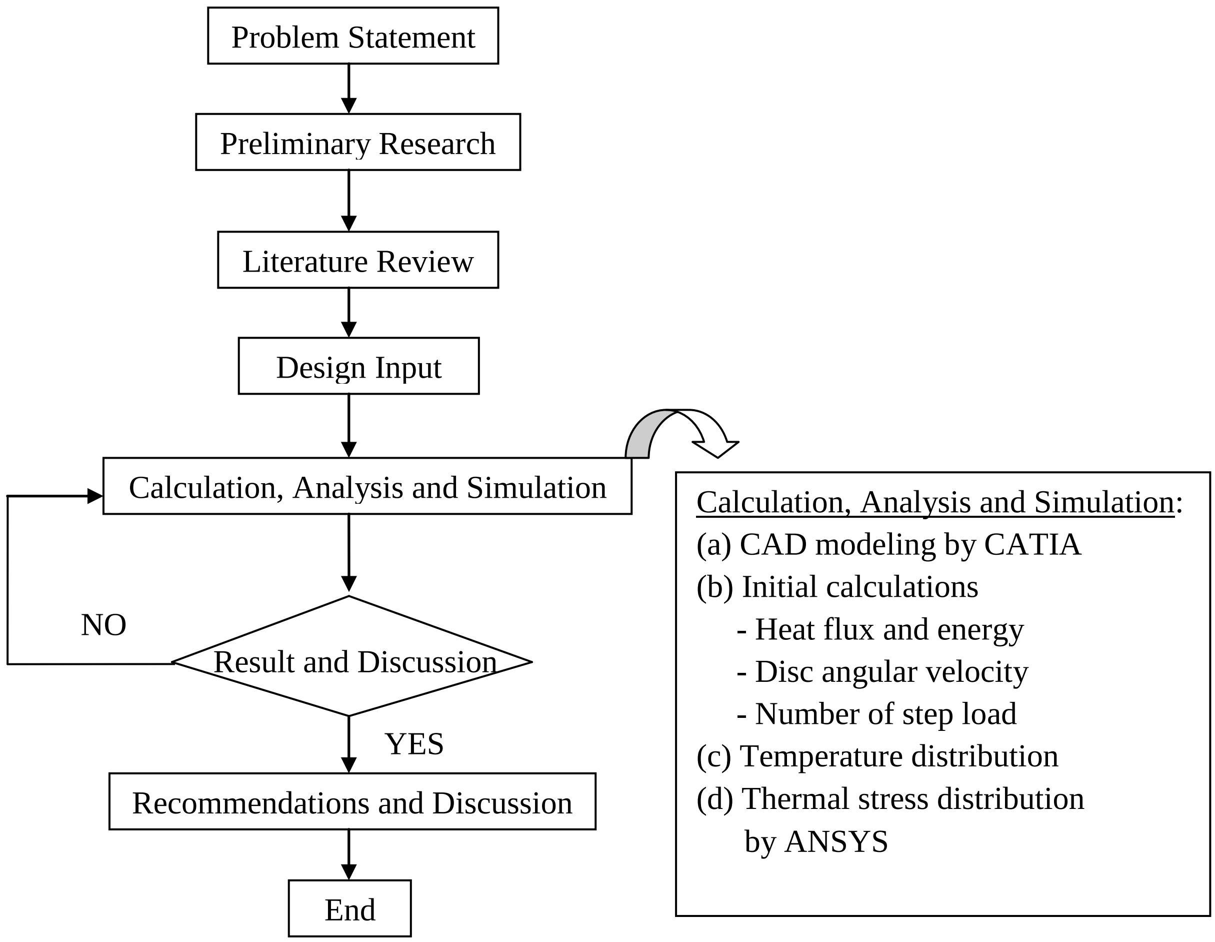

Figure 3.1: Methodology

3.2 DATA GATHERING

3.2.1 Vehicle Specifications

Table 3.1 contains the vehicle's specifications that are used in the analysis. Please refer to Appendix A for the full calculations of each vehicle's specification.

Table 3.1: Vehicle Specifications

No.	Parameter	Specification
1	Engine capacity	2.4 liter (2400 cc)
2	Maximum car weight	1950kg
3	Front and rear axle weight rating	a) Front gross axle weight rating: 1060kg b) Rear gross axle weight rating: 915kg
4	Weight ratio	a) Front ratio = $\frac{1060kg}{1950kg}$ = 0.54 b) Rear ratio = $\frac{915kg}{1950kg}$ = 0.46
5	Considering maximum car weight for analysis	1950kg
6	Front and rear wheel applied weight	Front wheel applied weight = 1053kg Rear wheel applied weight = 897kg
7	Weight applied on each disc brake surface (heavier weight applied to front wheel is considered)	263.25 kg
8	Wheel Diameter	658 mm

3.2.2 Disc Brake and Brake Pad Specifications

Actual disc brake dimensions and specifications are obtained for further analysis in order to ensure that the result for temperature and thermal stresses distribution is as close to the real application condition as possible. The specifications for disc brake and brake pad are shown in Table 3.2 and Table 3.3 as following. Besides, the material of the disc brake is of Grey Cast Iron (ASTM A48) and its properties are shown in Table 3.4.

Figure 3.2 Perforated Disc Brake

Table 3.2 Disc Brake Specifications

No.	Parameter	Dimension (mm)
1	Outer diameter	328
2	Inner diameter	220
3	Individual disc thickness	5.75
4	Ventilation thickness	16.0
5	Ventilation wide	6.0
6	Perforation diameter	8.0

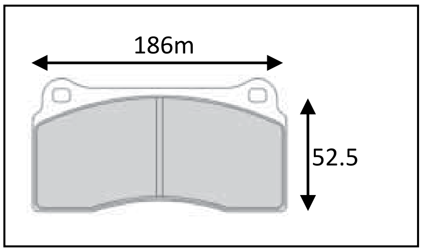

Figure 3.3 Brake Pad

Table 3.3 Brake Pad Specifications

No.	Parameter	Dimension (mm)
1	Thickness	17.5
2	Total length	186
3	Height	52.5

Table 3.4: Properties of Grey Cast Iron (ASTM A48)

No.	Property	Value
1	Specific heat, Cp	544 J/kg°C
2	Thermal conductivity, k	55 W/m°C
3	Density, ρ	7150kg/m^2
4	Coefficient of convection	50 W/m^2°C
5	Coefficient of thermal expansion, α	11.8 x 10^{-6} °/C^{-1}
6	Young’s modulus of elasticity, E	9.239 x10^{10} Pa
7	Poisson's ratio, v	0.26

3.3 DISC BRAKE DYNAMIC AND HEAT ANALYSIS

In this analysis, several assumptions and conditions are set to simplify the analysis and calculation as following:

- During the vehicle deceleration, the disc brake is assumed to be stationary while the brake pad rotates in counter-clockwise direction around it.
- Uniform pressure distribution by the brake pad onto the disc brake surface.
- Since a ventilated disc brake is being used as the sample with one side of the disc plate is asymmetrical to the other side, only one side of the disc plate is used in the analysis.
- The vehicle kinetic energy is 100% converted to heat energy with 95% of the total heat being absorbed by the disc while another 5% by the brake pad.
- Force distributed on one disc brake is equal to the total frictional force applied on the rubbing surface.
- Constant deceleration of the vehicle from initial speed of 150km/hr to stopping at 0.7 Gravity.

Based on the initial conditions and assumptions made, the value of the heat flux and time interval of each pad rotational movement or step are calculated to be set as input for ANSYS simulation. In the calculation, first of all the total stopping time and travelled distance is determined from the initial vehicle condition. Next, the disc brake initial angular velocity and acceleration is obtained to calculate the initial angular velocity of the next brake pad rotational movement. Then, the time interval between two pad rotational positions is calculated followed by the heat absorbed by the disc brake based on the vehicle kinetic energy calculation. Finally, the heat flux or heat transfer per unit area is obtained. These calculations will continue until the angular velocity of the rotating brake pad reached 0 rad/s. An example of the calculation is shown in Appendix B for the first brake pad movement and the following calculations till the final movement of brake pad is done with the help of Microsoft Excel as shown in Appendix C.

3.3.1 Justification of Selected Parameter for Analysis Condition

In the analysis of the thermal stresses that arise within the vehicle's disc brake due to the braking mechanism, it is assumed that the constant deceleration experienced by the vehicle prior to stopping to be of 0.7 gravity. Throughout the analysis in this project, the parameters chosen including the dimensions of disc brake and brake pad, vehicle specifications and also the vehicle operating conditions are referred to the real available parameters in order to ensure the accuracy of the analysis to be as close to the real working conditions. This also includes the optimum choice of the vehicle constant deceleration of 0.7 gravity based on the maximum braking specification of the selected vehicle model to create a worst case braking scenario in order to study the maximum effect of braking on the development of thermal stresses. The justification of the chosen constant deceleration value can be referred to the following estimation.

Maximum deceleration capability of vehicle obtained from two testing sources:

i. <u>Testing one (referred to www.carwale.com/Research)</u>

   Minimum vehicle stopping distance = 52.87m, initial speed at 100km/hr.

   $v^2 = u^2 + 2\ a\ s$

   $0^2 = (27.78 m/s)^2 + 2\ a\ (52.87\text{m})$

   $a = -7.2972\ \text{m}/s^2$

   in gravity fraction = $\frac{-7.2972\text{m}/s^2}{-9.81\text{m}/s^2}$ = <u>0.744 gravity</u>

ii. <u>Testing Two (referred to http://productsearch.rediff.com/productdetail)</u>

   Minimum vehicle stopping distance = 49.10m, initial speed at 100km/hr.

   $v^2 = u^2 + 2\ a\ s$

   $0^2 = (27.78 m/s)^2 + 2\ a\ (49.10\text{m})$

   $a = -7.875\ \text{m}/s^2$

   in gravity fraction = $\frac{-7.875\text{m}/s^2}{-9.81\text{m}/s^2}$ = <u>0.80 gravity</u>

Thus, from the analysis, vehicle's constant deceleration is justified by choosing value of 0.7gravity as the initial condition input because this value is slightly lower than the maximum deceleration that this vehicle can achieve in reality.

3.3.2 Dynamic and Heat Energy Analysis

From the dynamic calculation of the brake pad rotational movements around the disc brake until it stopped, an angular velocity versus time graph is plotted as shown in Figure 3.4 below. It shows the time taken by the vehicle starting with the initial angular velocity of the brake pad at 126.66 rad/s decreasing to 0 rad/s in 6.01 seconds. In other word, this is the time taken for complete conversion of the vehicle's kinetic energy into heat energy by the first law of thermodynamics. Furthermore, from the dynamic calculation, the brake pad experienced 367 rotational steps before it came to complete stop. Also from the graph, the angular velocity of the brake pad is decreasing linearly with time due to the constant deceleration of the vehicle at 0.7 Gravity.

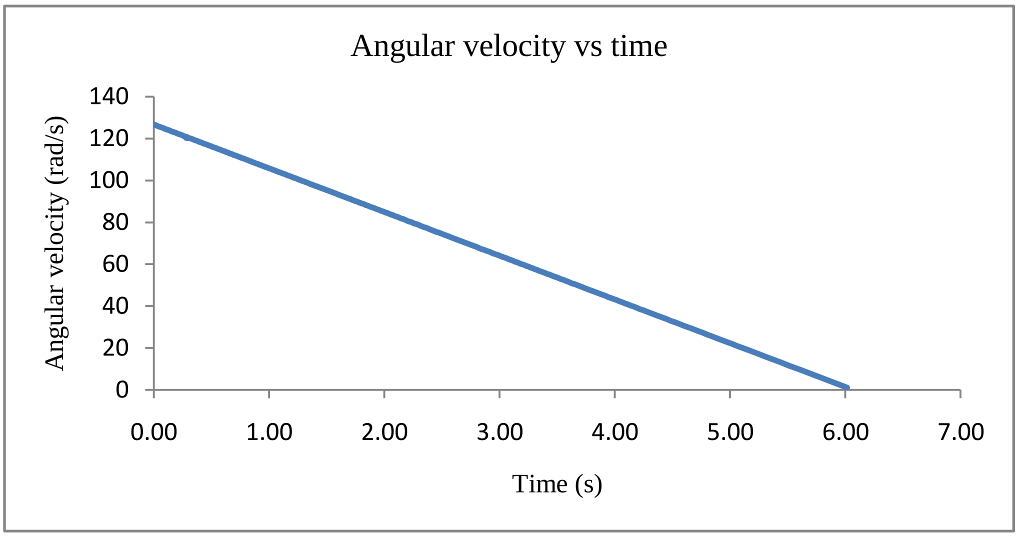

Figure 3.4: Angular Velocity versus Time

As the vehicle kinetic energy decrease due to the decreasing vehicle speed, heat energy is slowly building up from the conversion of the kinetic energy to heat energy by the frictional force between the surfaces of disc brake and pad. In this analysis, all the kinetic energy is assumed to be converted into heat energy with 95% of it is absorbed by the disc brake and another 5% by the brake pad. Following Figure 3.5 shown the graph of accumulative heat energy versus the time taken by the vehicle to stop. The plotted curve gave a parabolic response with moderate increase of the heat energy generation at the beginning and decreases with time where the total accumulated heat energy is 217121.05 Joule.

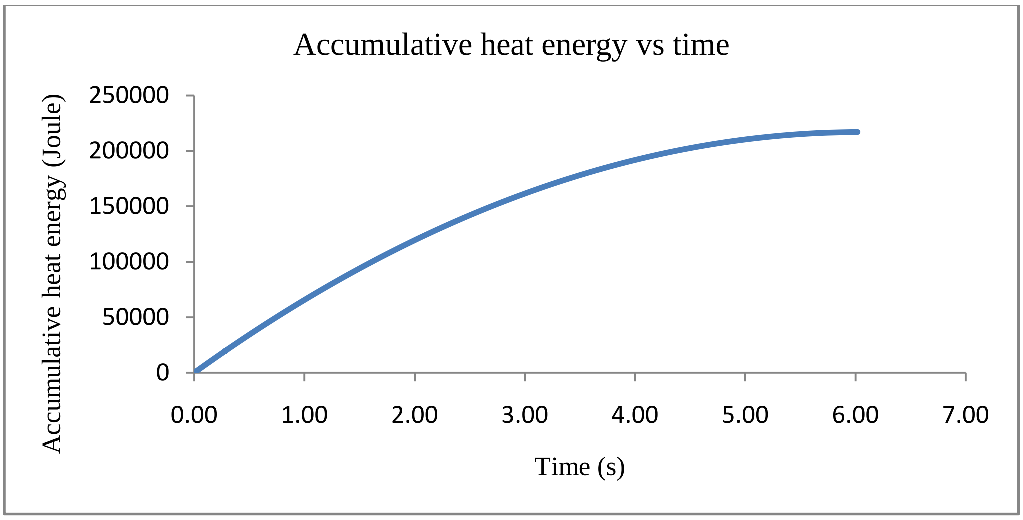

Figure 3.5: Accumulative Heat Energy versus Time

3.3.3 Heat Flux Generation

Heat flux is the measurement of heat transfer per unit area. It is the amount of heat absorbed by the disc brake surface per unit time and Figure 3.6 shown the corresponding heat flux versus time graph from the start of the braking force application of the pad onto the disc until the disc stopped rotating. The graph shown the highest heat flux value of 9226731.6 KW/m^2at the beginning of the analysis due to the higher angular velocity of the disc brake at that moment, and heat flux value linearly decreases with time as the vehicle decelerated constantly at 0.7 Gravity.

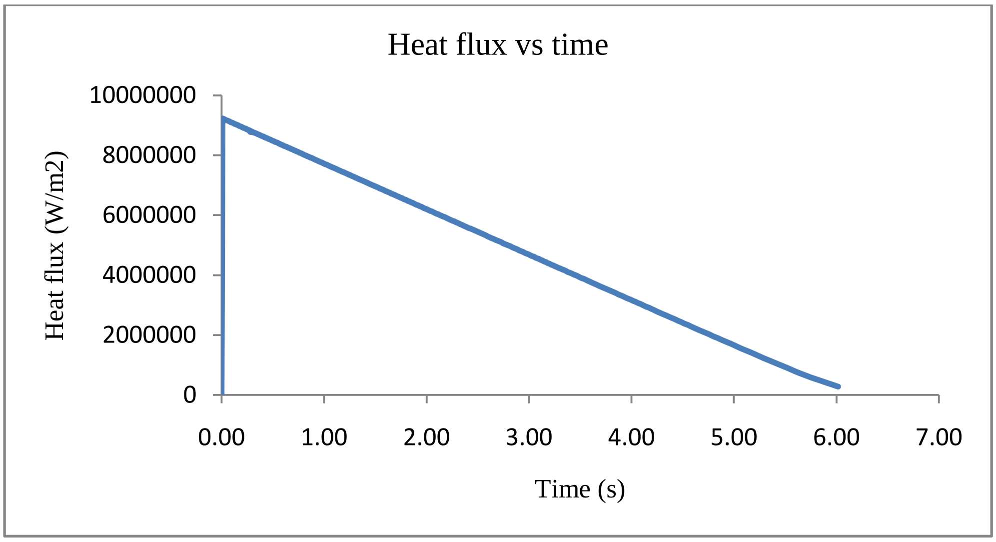

Figure 3.6: Heat Flux versus Time

3.4 DISC BRAKE MODELING

The three dimensional model of the disc brake is generated by using CATIA, a computer aided design software according to the specific disc brake dimensions. For the thermal stresses analysis, only one plate of the disc brake will be used because both disc plates are asymmetrical to each other and assumption is being made that both sides of the disc plate experience same amount of force by the brake pad and thus having the same temperature distribution allowing asymmetric analysis. In order to ensure that the analysis results are as accurate as the real condition, the vents which connect two disc plates together are also included into the modeled disc brake.

This model is transferred to ANSYS for finite element analysis where heat flux will be applied on one side of this disc brake as the brake pad rotates around the disc. The heat flux is transfer to the surface of the disc brake according to the rotary position of the pad and the brake pad covers 60° of the disc brake surface area at a time. Thus, the area covered by the pad will experiences the transfer of heat flux to the surface while leaving the rest of 300° without any heat flux application but convection to the surrounding. Furthermore, there will be no heat transfer at the surface of the sliced vents where an adiabatic condition is assumed. In order for 60° covered area to be selected in the ANSYS for heat flux application, the disc brake models have been divided into 6 individual parts in the CATIA and are glued into one single volume in ANSYS.

In order for comparisons to be made between perforated and non-perforated disc brakes, both types of disc brakes are being modeled and similar tests of temperature and thermal stresses distribution are carried out in order to investigate the trend for each disc brake and further conclude on how perforation will affects the performance of the disc brake and the vehicle in general. The non-perforated disc brake model is modified based on the dimensions of perforated disc brake with the different in the absence of perforation holes. The isometric, top and bottom views of the modeled perforated disc brake volume are shown is Figure 3.7, 3.8 and 3.9 respectively while the isometric, top and bottom views of the modeled non-perforated disc brake are shown in Figure 3.10, 3.11 and 3.12 respectively.

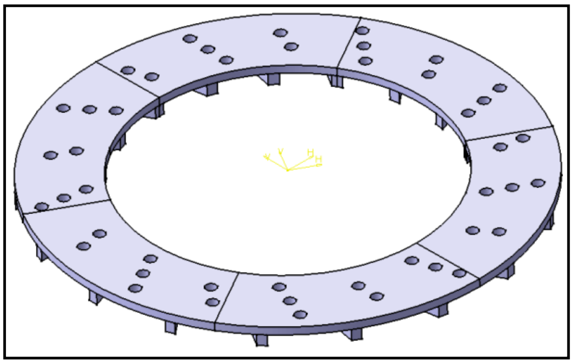

Figure 3.7: Isometric View of Perforated Disc Brake

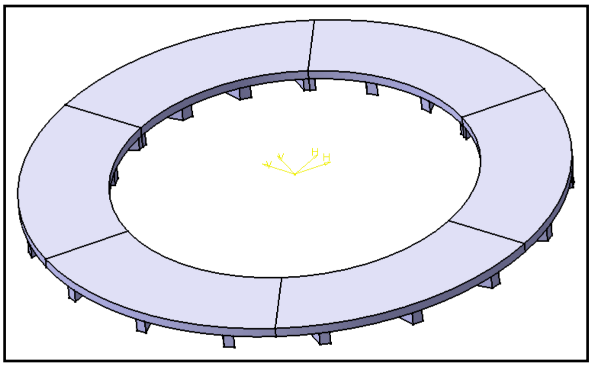

Figure 3.10: Isometric View of Non-Perforated

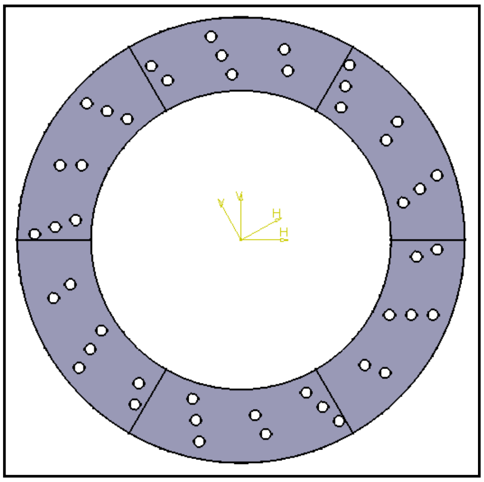

Figure 3.8: Top View of Perforated Disc

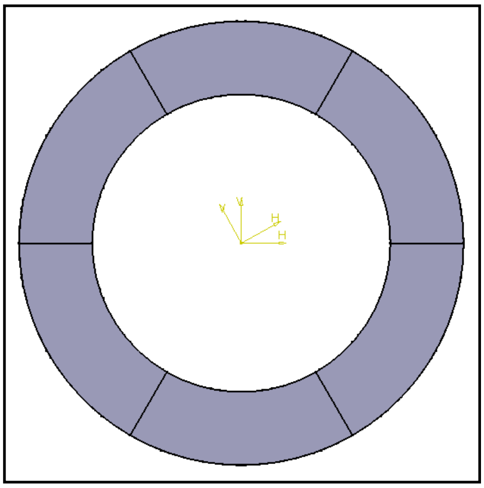

Figure 3.11: Top View of Non-Perforated Disc Brake

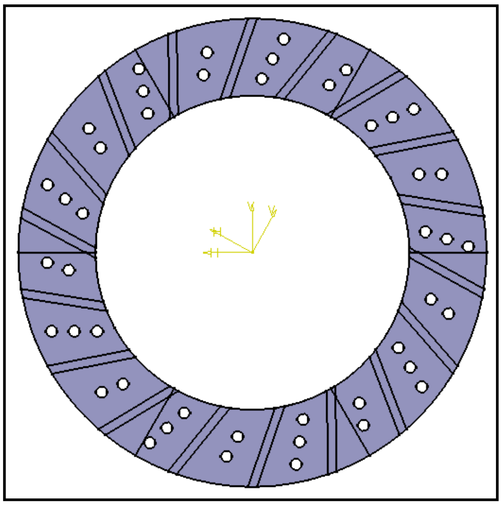

Figure 3.9: Bottom View of Perforated Disc Brake

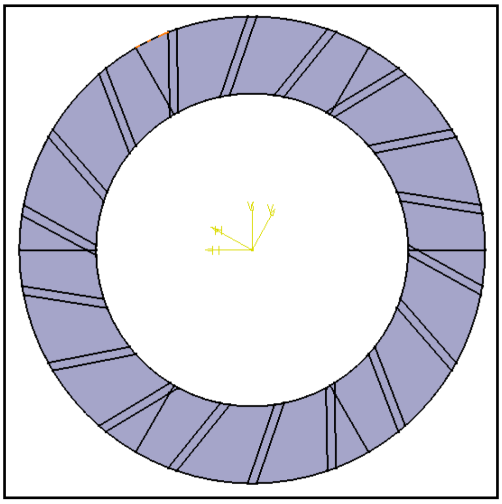

Figure 3.12: Bottom View of Non-Perforated Disc

3.5 FINITE ELEMENT MODELING

Finite element analysis is the best method that can be used in this project to investigate the behaviors of thermal stresses of the disc brake. This is because finite element method is a good choice for solving partial differential equations over complicated shapes or subjects such as the perforated disc brake, where the subject will reacts with changes in its physical properties. Besides, finite element method allows precise simulation and computation over the entire body of the subjects. In the investigations of the disc brake behaviors under the influences of heat flux, the modeled disc brakes are meshed by using the ANSYS software to prepare them for finite element analysis by dividing the model volume into smaller elements.

Since the simulation is being carried out with the use of three dimensional models, element type of SOLID 87 is chosen to give the best meshing attributes to the disc brake and the material properties are defined as the properties of grey cast iron in shown in Table 3.4. This is because the quality of the volume meshing will directly affects the accuracy of the finite element simulation results. While for the analysis of thermal stress, element type of BRICK SOLID 186 is chosen. Both the volumes of perforated and non-perforated disc brakes are meshed in ANSYS with 39747 elements and 35986 elements generated for perforated and non-perforated disc brake respectively. The meshing patterns of the perforated and non perforated disc brake are shown in following figures in section 3.5.1 and 3.5.2.

3.5.1 Meshing of Perforated Disc Brake

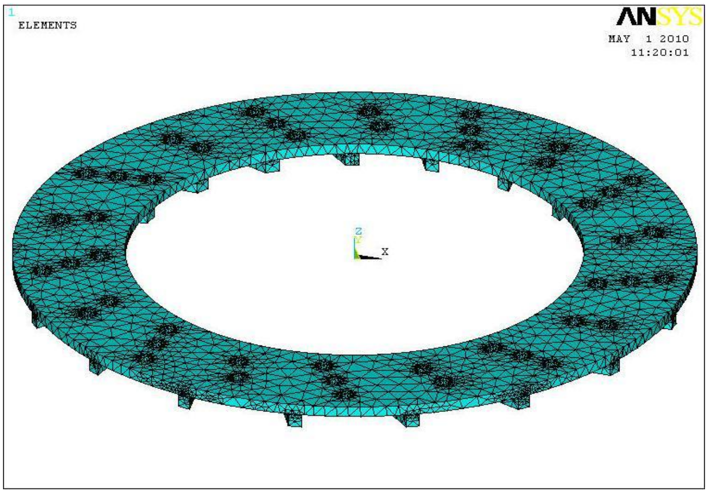

Figure 3.13: Isometric view of Perforated Disc Brake Meshing

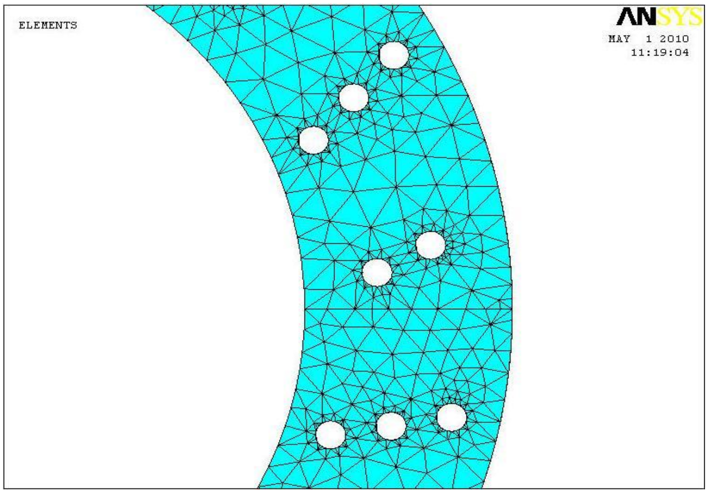

Figure 3.14: Detailed view of Perforated Disc Brake Meshing

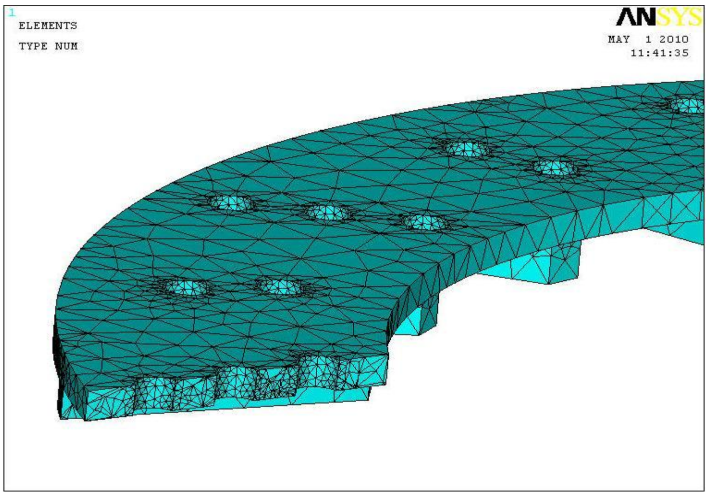

Figure 3.15: Cross Section view of Perforated Disc Brake Meshing

3.5.2 Meshing of Non-Perforated Disc Brake

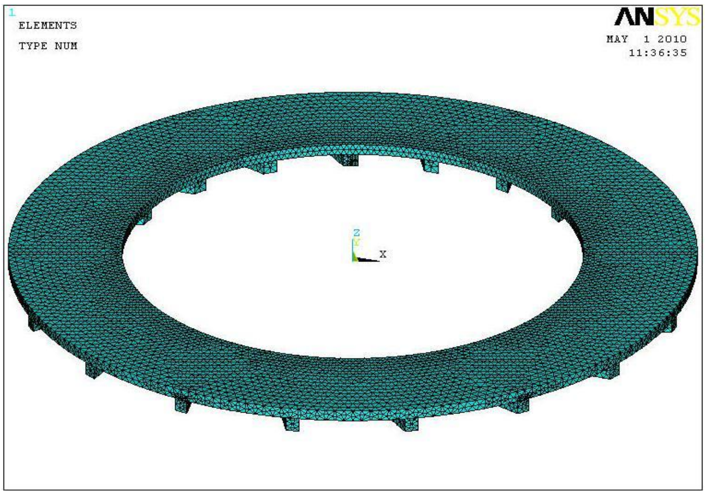

Figure 3.16: Isometric view of Non-Perforated Disc Brake Meshing

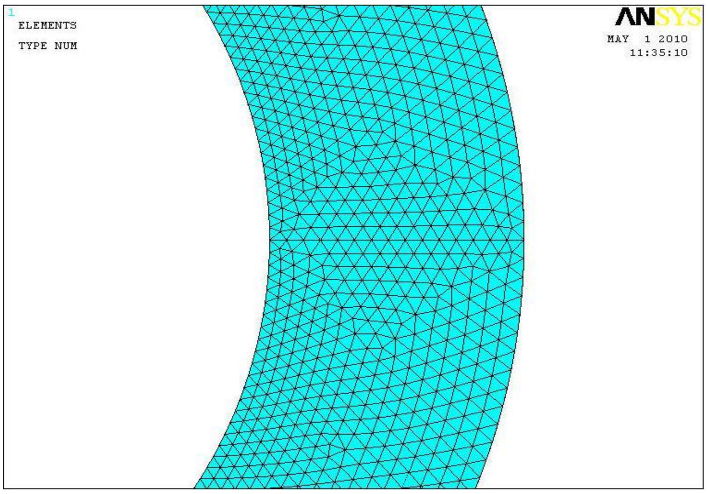

Figure 3.17: Detailed view of Non-Perforated Disc Brake Meshing

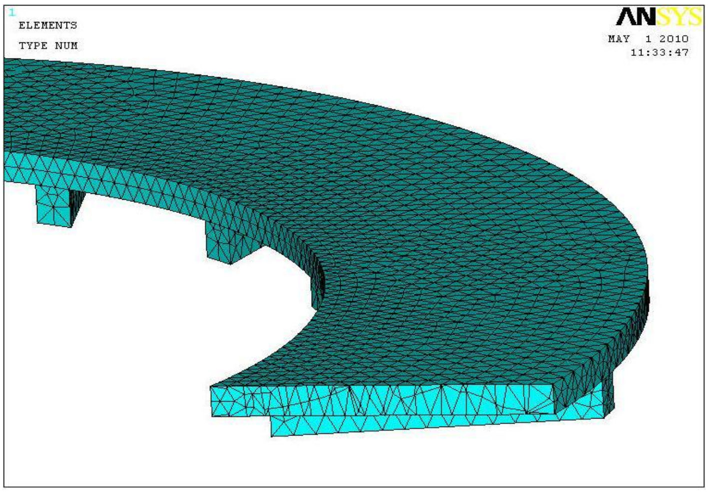

Figure 3.18: Cross Section View of Non-Perforated Disc Brake Meshing

3.6 SIMULATION INITIAL CONDITIONS AND PARAMETERS

Before simulation processes can be run to test the disc brakes, there are few initial conditions and parameters that need to be defined on the finite element volumes, some of the parameters and assumption made are:

- Initial temperature of the disc brake volume is 30°C.
- Ambient temperature is taken to be 25°C room temperature.
- Coefficient of convection is 50 W/m^2°C.
- The bottom surface of the ventilation joints (vents) is assumed to be adiabatic.
- Heat flux applied to the disc brake's surface is uniform throughout the area.
- No constrain will be defined for the disc brake on the temperature distribution analysis but for thermal stress and thermal expansion analysis, constrain is defined at the inner diameter surface of the disc brake.

As calculated in the disc brake kinetic calculation section, there are 367 thermal load steps before the disc brake come to complete stop. Since the pad only covers an area of 60° from the whole disc brake area, there will be 367 rotating motion of the break pad with each pad position having different values of heat flux and time interval as per calculated. On the other hand, for area which is not covered by the pad, cooling process through heat convection will take place. Each thermal load step will be solved by ANSYS simulation for temperature distribution analysis and the result from the previous load step will be used as the initial condition input for the next thermal load step. Next, for thermal stress analysis, the generated temperature distribution will be used as the input for their analysis. This process will be repeated for 367 times until the pad stops.

Since the finite element analysis using ANSYS requires 367 moving load steps to be defined and being fed as inputs, ANSYS command language is generated using C++ programming software in order to simplify these steps. Besides, this method allow correction to be make onto the command language without having to repeat the whole input defining process manually and it saves time. The example of the written programming codes in generating ANSYS command language is shown in Appendix D. The total simulation time is 5.99 s.

CHAPTER 4

RESULT AND DISCUSSION

4.1 DISC BRAKE TEMPERATURE DISTRIBUTION

Disc brake surface and body temperature increases due to the heat flux generated by the frictional contact with the brake pad. In order to investigate the increase of disc brake temperature at different thickness, four nodes labeled as A, B, C and D have been chosen along its thickness. Node A is situated at the contact surface between the disc and the pad while node D is situated at its bottom surface with node B and C come in between. The plotted nodes temperatures again the running time of 5.99 s for perforated and non-perforated disc brake are shown in Figure 4.1 and 4.2.

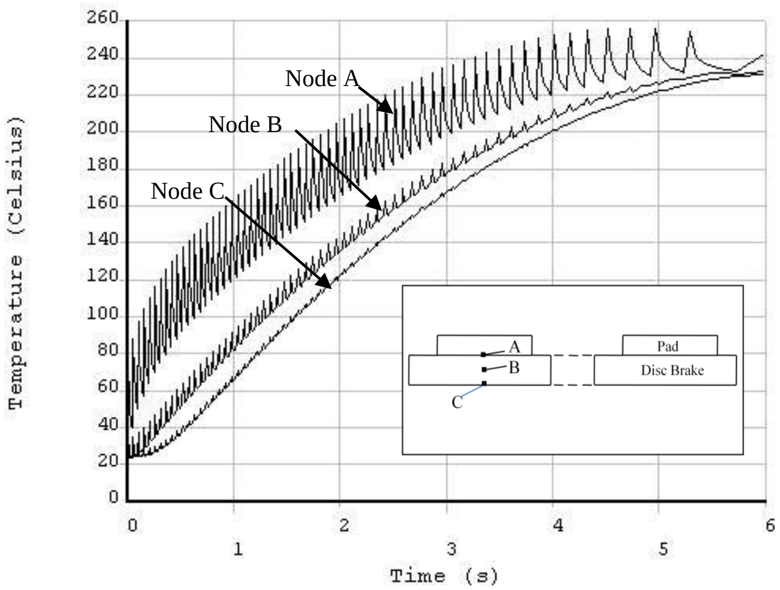

Figure 4.1: Temperature History at Nodes A, B & C (Perforated Disc Brake)

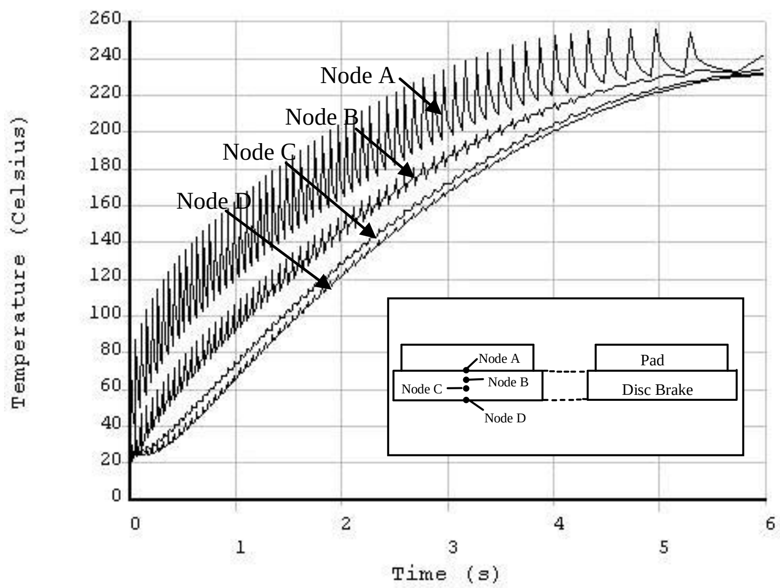

Figure 4.2: Temperature History at Nodes A, B, C & D (Non-Perforated Disc Brake)

For both perforated and non perforated disc brake, the temperature is highest at node A because node A located at the frictional surface between the pad and disc brake where heat flux is at its maximum. The fluctuation of temperature throughout the analysis time is due to the repeating heating (heat flux) and cooling (convection) processes at the disc brake's surface. This fluctuating pattern shows similarity to the fluctuating surface temperature of disc brake in the research done by C.H. Gao & X.Z. Lin [10]. Furthermore, the fluctuating pattern is more obvious for node A because this node is situated at the surface which experienced thermal convection with the chance to release greater amount of heat compared to other nodes position. By referring to Figure 4.1 above, the highest temperature achieved by the perforated disc brake is 256.4 °C at time 4.722 of node A. While the highest temperature achieved by node B and C are 233.8 °C and 231.2 °C respectively. The temperature of node B and C are lower than node A because they are situated further from thermal source which is the heat flux generated by the frictional surface.

By referring to Figure 4.2, the highest temperature achieved by the non - perforated disc brake is 256.4 °C at time 4.686 seconds of node A. While the highest temperature achieved by node B, C and D are 233.7 °C, 231.9 °C and 231.2 °C respectively. By comparing both disc brakes, the maximum temperature produced is almost the same which can be verified by referring to the experiment by M.Eltoukhy [11] regarding simulation of heat generation problem. Thus attention will be further focusing on the temperature distribution within disc brake body.

4.1.1 Temperature Distribution along Frictional Surface

Temperature distribution can also be investigated by looking into its distribution along the frictional surface between disc brake and brake pad. Figure 4.3 shows the A – A' path along the radial distance of the disc brake's surface. This path is selected along the surface of solid cross section for the perforated disc brake. The temperature at different time during the simulation period is recorded in order to investigate the temperature distribution at these particular times. Temperature distribution along the frictional surface for perforated disc brake is shown in Figure 4.4 and non perforated disc brake in Figure 4.5. The temperature distribution along the surface increases with the time until a maximum value at time just before the end of simulation period. This is due to the increment in the accumulated frictional heat flux to the disc brake's surface.

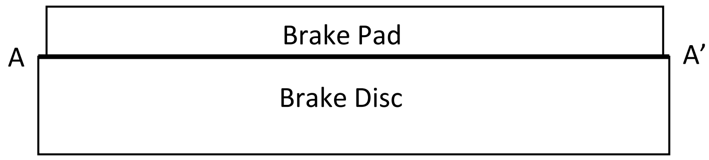

Figure 4.3: A – A' Path along the Radial Distance of Disc Brake

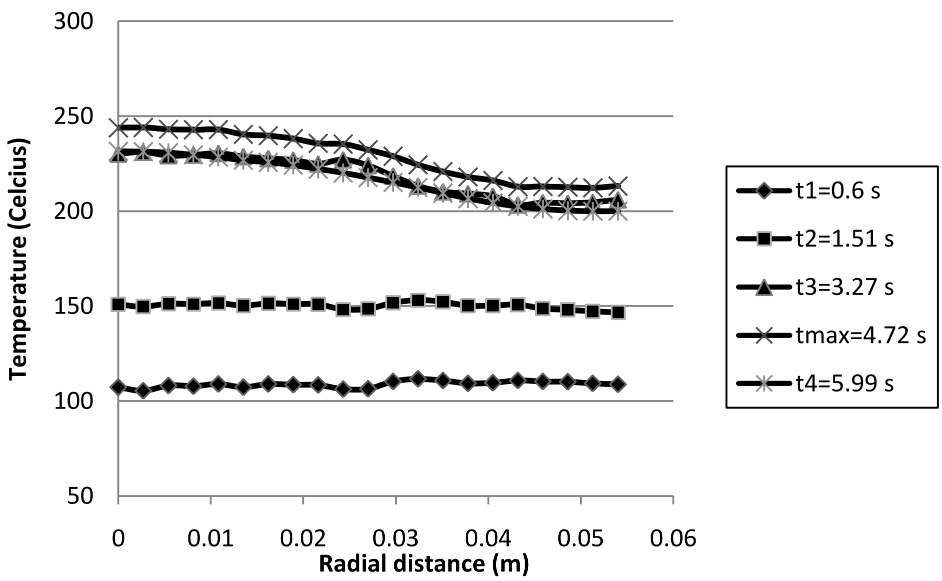

Figure 4.4: Temperature Distribution along Path A – A' for Perforated Disc Brake at Different times

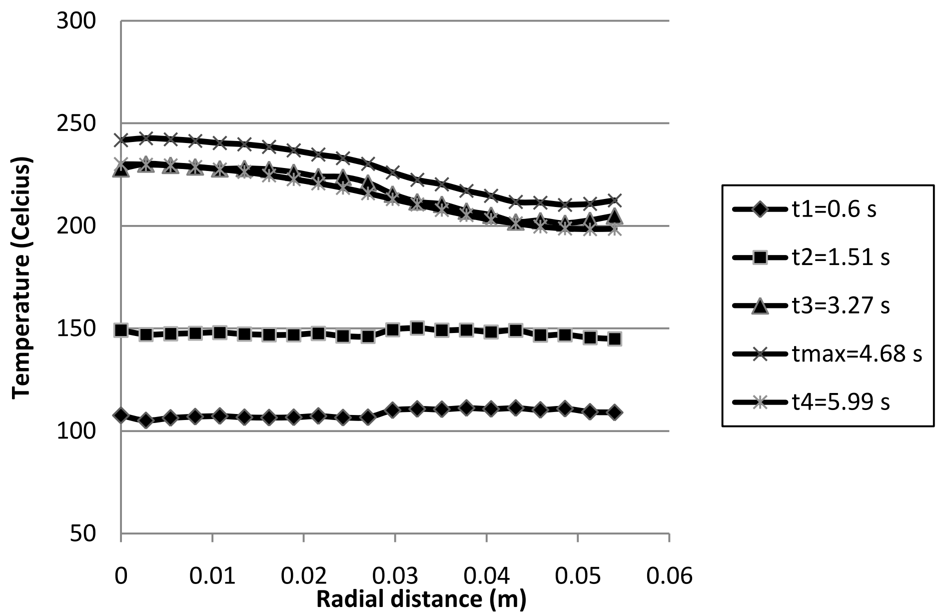

Figure 4.5: Temperature Distribution along Path A – A' for Non Perforated Disc Brake at Different times

A more detailed temperature distributions are obtained by specifying path A – A', B – B' and C – C' which are the paths along the disc brake's surface, mid way along of disc brake's thickness and along bottom of the disc brake respectively as shown in Figure 4.6. Further comparison is made for both disc brakes at the time where the temperature reached its maximum for both cases, 4.72 seconds for perforated disc and 4.68 seconds for non perforated disc as shown in Figure 4.7.

The plotted temperature distribution curves show that the distribution patterns for all three paths for perforated and non perforated discs are almost the same pattern with small decrease in temperature at the outer radial distance. This is largely because they are all situated perpendicular to the heat source with path A – A' received the highest magnitude of frictional heat flux at the surface followed by path B – B' and path C – C', which explain why the temperature distribution for path A – A' is the highest, path C – C' the lowest and path B – B' comes in between. Through the comparison of temperature distribution for perforated and non perforated disc brake, both show similar distribution for all three paths.

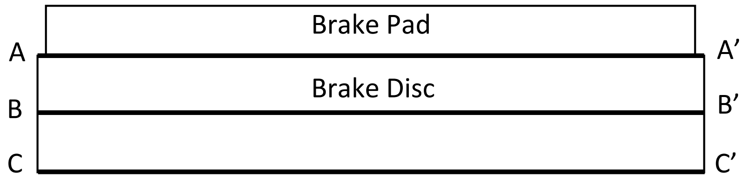

Figure 4.6: A – A’, B – B’ and C – C’ Paths along the Radial Distance of Disc Brake

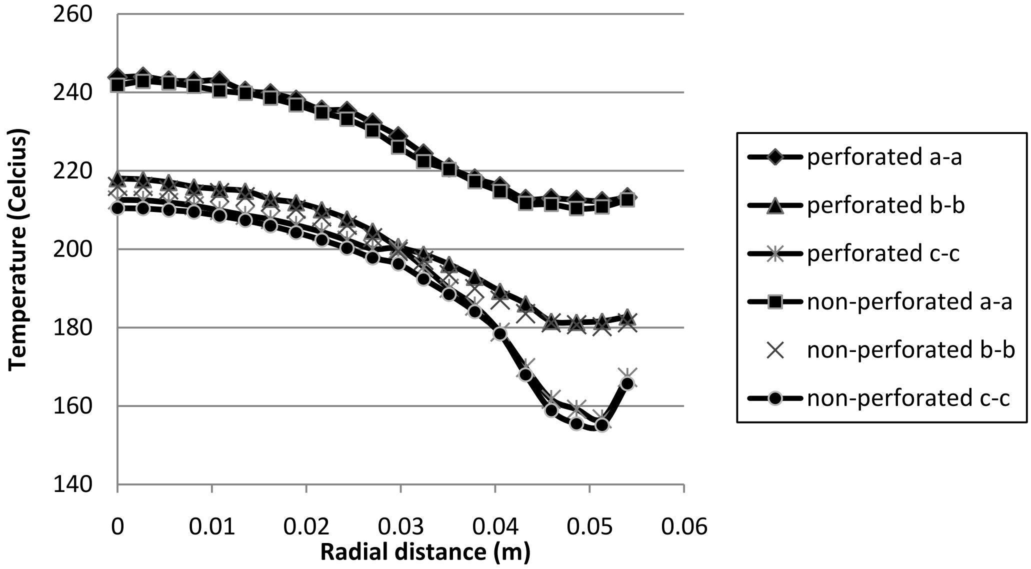

Figure 4.7: Temperature Distribution along Path A-A’, B-B’ and C-C’ for Perforated and Non Perforated Disc at Time 4.72 Seconds and 4.68 Seconds Respectively

4.1.2 Temperature Distribution across the Cross Section

Temperature distribution within the disc brake body is analyzed by creating a slicing plane along the perforated holes to compare the temperature distribution between perforated and non perforated disc brake. Figure 4.8 and 4.9 illustrate how the temperature is being produced and distributed at the end of braking process, after 5.99 seconds.

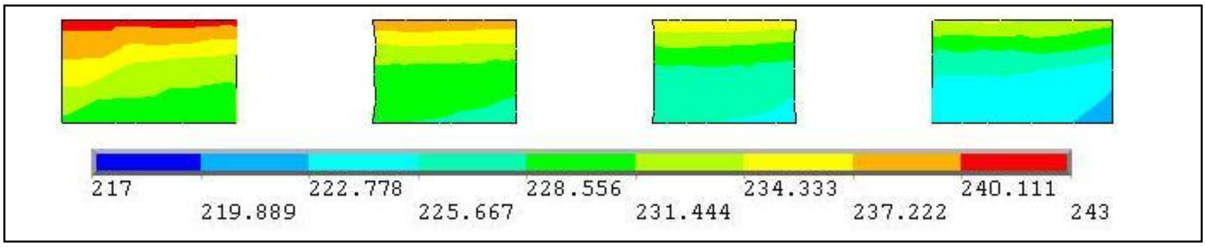

Figure 4.8: Cross Section Temperature Distribution (Perforated Disc Brake), Time 5.99s

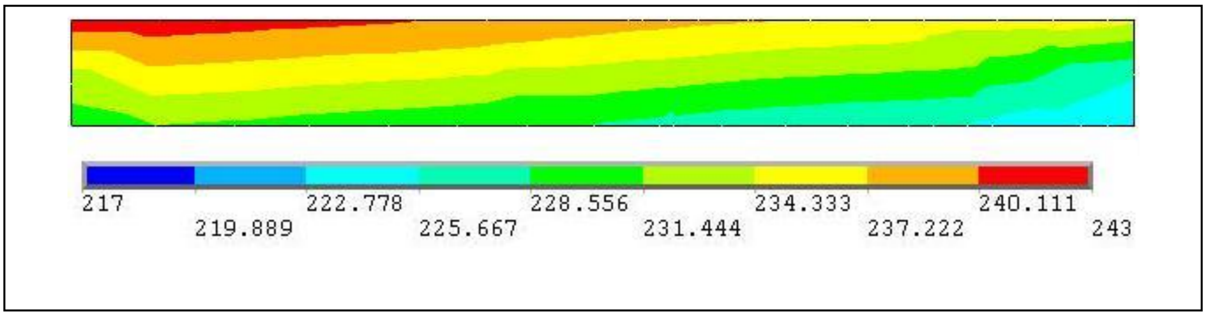

Figure 4.9: Cross Section Temperature Distribution (Non Perforated Disc Brake), Time 5.99s

Both Figure 4.8 and 4.9 provide a better illustration of temperature distribution across the disc brake and by comparing both disc brakes, the perforated disc seen to provide better results as far as the temperature distribution is concerned as compared to non perforated disc. Although earlier analysis shown that the maximum temperature produced by both disc brakes is almost the same, the temperature distribution varies for both disc brake. Figure 4.8 shows that perforated holes contributed to better temperature distribution by having less red to yellow colored region within its cross section, giving better cooling effect although the maximum temperature is the same for both cases. Refer to Figures 4.10 and 4.11 from Section 4.1.2.1 and 4.1.2.2 respectively for cross section temperature distribution for various braking period.

4.1.2.1 Temperature Distribution across Cross Section for Perforated Disc

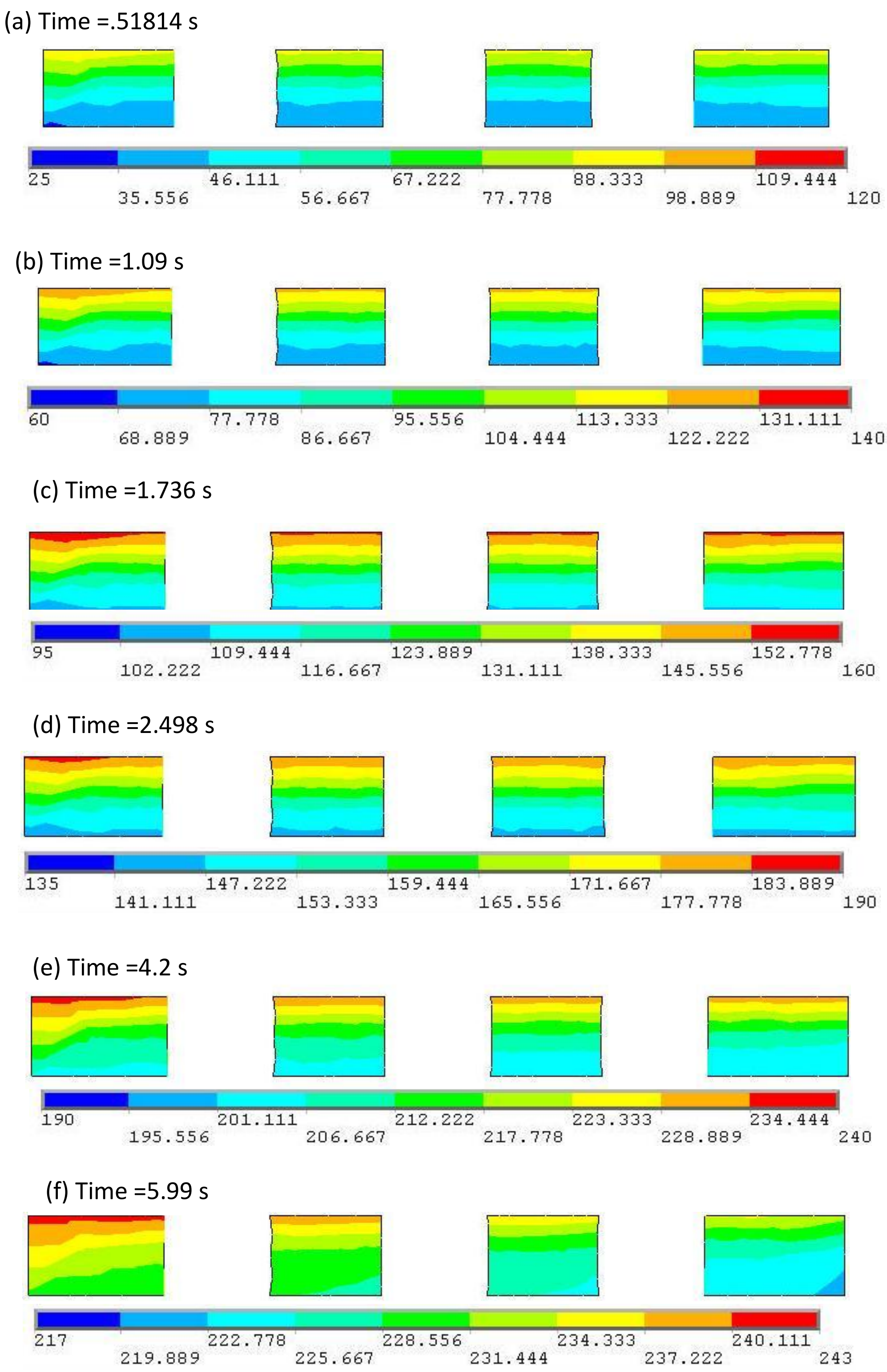

Figure 4.10: Temperature Distribution across Cross Section for Perforated Disc at Different Set of Time

4.1.2.2 Temperature Distribution across Cross Section for Non Perforated Disc

(a) Time =.51814 s

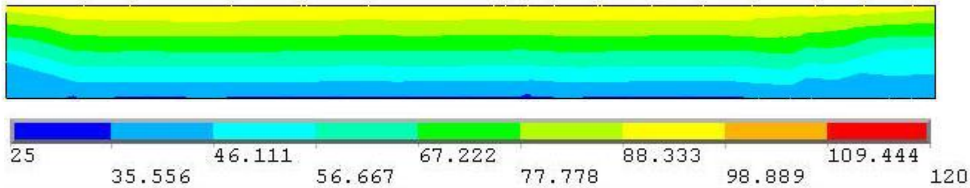

(b) Time =1.09 s

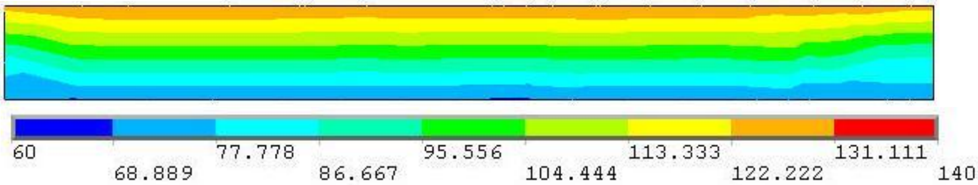

(c) Time =1.736 s

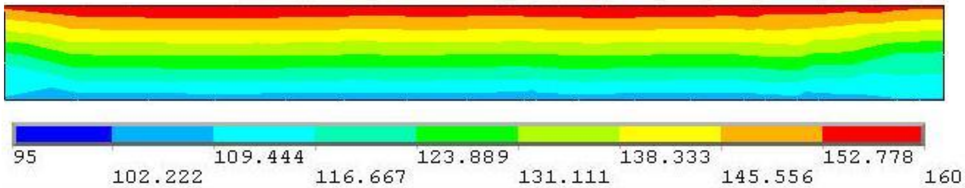

(d) Time =2.498 s

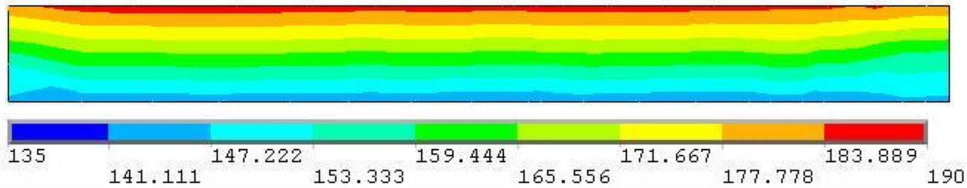

(e) Time =4.2 s

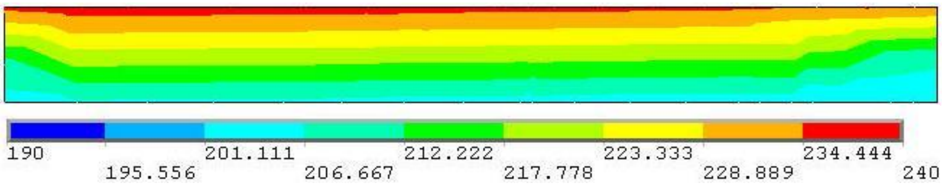

(f) Time =5.99 s

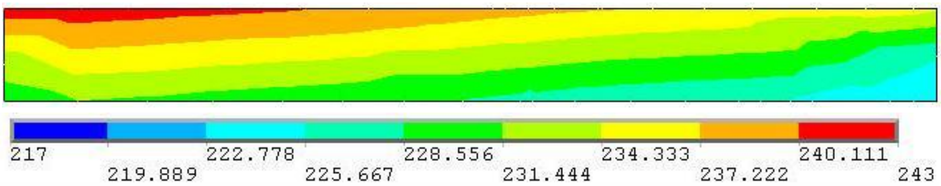

Figure 4.11: Temperature Distribution across Cross Section for Non Perforated Disc at Different Set of Time

4.1.3 Temperature Contour

Another interesting observation is the overall surface temperature distribution of both disc brakes. It gives a bigger picture of the effects of perforation on the temperature distribution. Figure 4.12 below shows the top surface temperature distribution at time 5.99 seconds. Refer to Appendix E for temperature distribution (disc brake's top view) in various braking period.

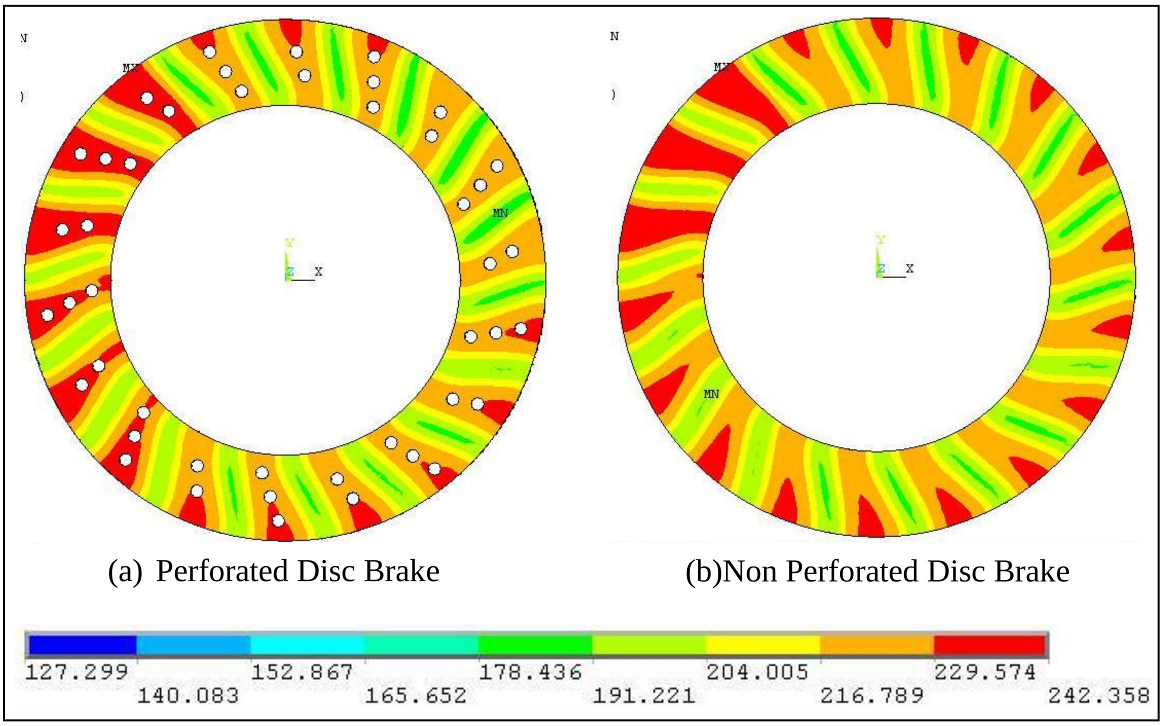

Figure 4.12: Top Surface Temperature Distribution, Time 5.99s

The overall top surface temperature distribution also shows that the perforated disc brake has better temperature distribution because it has less high temperature region (red colored) over the whole surface as compared to non perforated disc brake. And it is noticed that the high temperature regions concentrated around the outer parameter of both disc brakes. Besides, it can also be concluded that the vents connecting two disc plates for ventilated disc brake eventually helped in the cooling process of the disc brake as shown Figure 4.13. The vents (blue colored regions) provide larger surface area for heat convection to the ambient environment and thus lower the surface temperature.

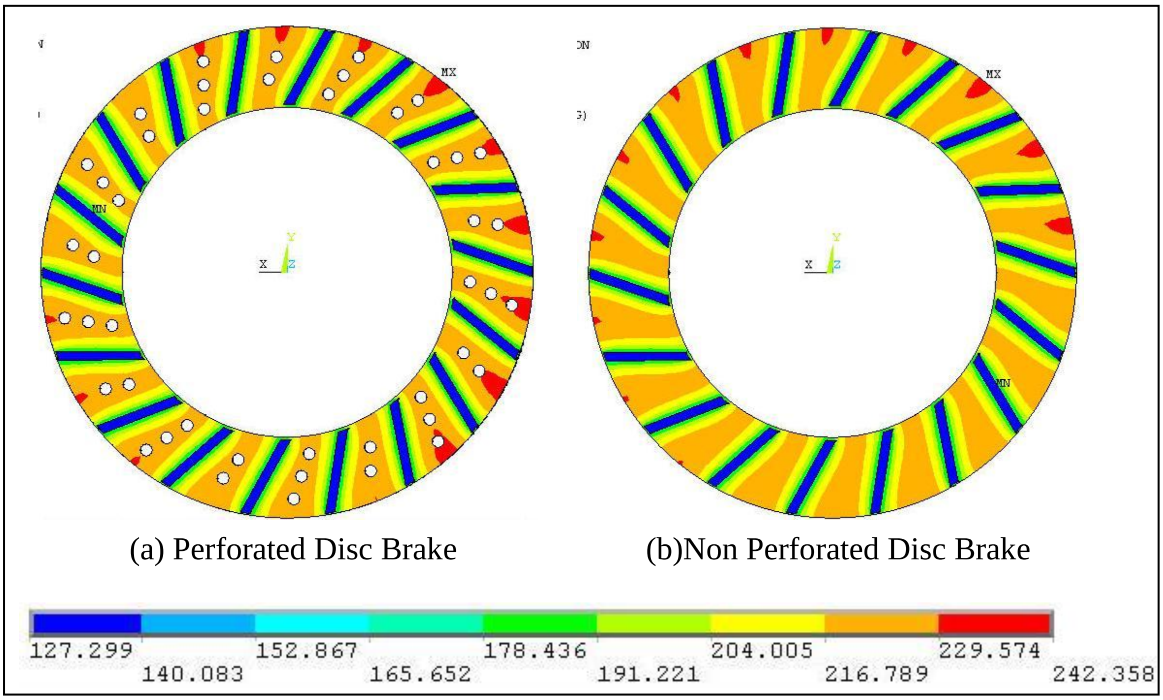

Figure 4.13: Bottom Surface Temperature Distribution, Time 5.99s

4.2 DISC BRAKE THERMAL STRESS DISTRIBUTION

The temperature rise on the contact surface between brake pad and disc brake will contribute to the development of thermal stress on the disc brake body. This thermal stress arises due to the compression from the forbidden expansion of the disc brake when the internal surface of the disc is constrained as illustrated in Figure 4.14.

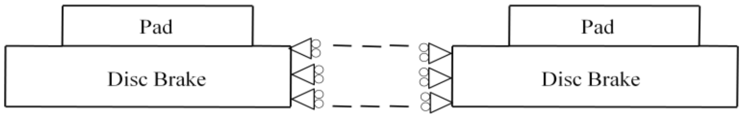

Figure 4.14: Disc Brake Constrained Area

The thermal stress on disc brake surface and body increases due to the increase in the temperature caused by absorbed heat flux. In order to investigate the increase of disc brake's thermal stress at different thickness of the disc, four nodes labeled as A, B, C and D have been chosen along its thickness, similar to temperature distribution analysis. Node A is situated at the contact surface between the disc and the pad while node D is situated at its bottom surface with node B and C come in between. The plotted thermal stress history for perforated and non-perforated disc brake are shown in Figure 4.15 and 4.16.

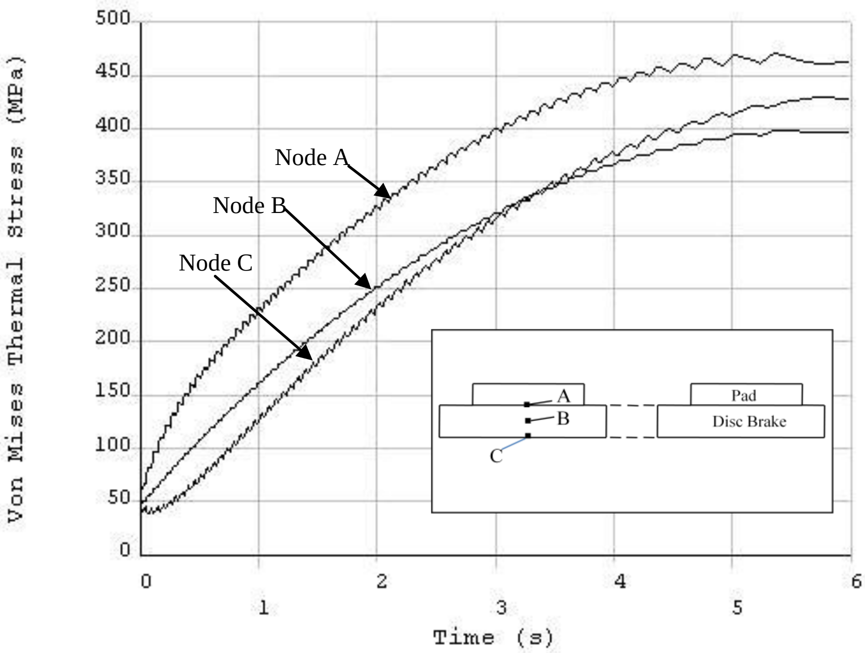

Figure 4.15: Von Mises Thermal Stress History (Perforated Disc Brake)

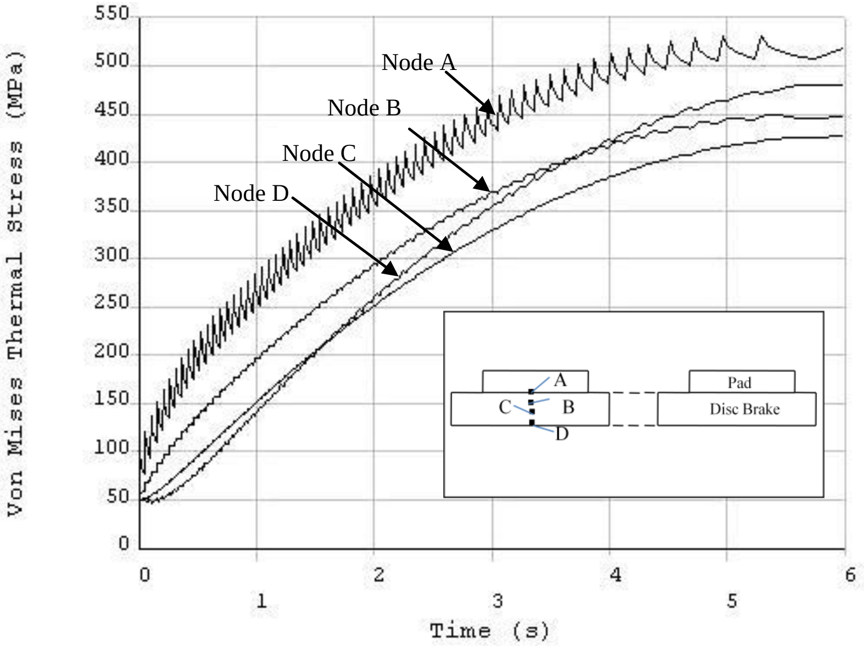

Figure 4.16: Von Mises Thermal Stress History (Non-Perforated Disc Brake)

For both perforated and non perforated disc brake, the thermal stress is the highest at node A because node A is located at the frictional surface between the pad and disc brake where heat flux and subsequently temperature rise is at their maximum. The fluctuation pattern of thermal stress especially at node A as shown in Figure 4.15 and 4.16 is due to the repeating heating (heat flux) and cooling (convection) processes at the disc brake's surface, which is similar to the fluctuation of the node A's temperature in Figure 4.1 and 4.2. This thermal stress fluctuating pattern shows similarity to the fluctuation of disc brake surface's thermal stress in a research done by Pier Francesco Gotowicki, Prof. Vinzenco Nigrelli & their team [14]. As the result of frictional action on the disc brake surface, disc brake's temperature will increase causing the disc brake to expand. But due to the applied constrain, stress is developed. Since the inner part of the disc brake surface is constrained as shown in Figure 4.14, the material of the disc tends to expand toward the outer side of the disc. Thus, Node A will experiences expansion force while node D experiences compaction force.

For perforated disc, the highest thermal stress achieved is 470.67 MPa at node A, while the highest thermal stress achieved by node B and C are 398.68 MPa and 429.18 MPa respectively. The thermal stress of node B and C are lower than node A because they are situated further from thermal source but at the end of the braking time the thermal stress value for node C increase closing to node A's thermal stress value due to the increase of the compaction stress at node C. While for the non perforated disc brake, the highest thermal stress achieved is 531.14 MPa at node A. And the highest thermal stress achieved by node B, C and D are 449.54 MPa, 425.13 MPa and 480.45 MPa respectively. The thermal stress of node B, C and D are lower than node A because they are situated further from thermal source but at the end of the braking time the thermal stress value for node D increase closing to node A 's thermal stress value due to the increase of the compaction stress at node D. By comparing both disc brakes, the maximum thermal stress produced by perforated disc brake is lower than the non perforated disc. Thus attention will be further focusing on the thermal stress distribution within disc brake body to compare both disc brakes by looking at their overall thermal stress distribution instead of at few selected nodes.

4.2.1 Surface Thermal Stress Distribution

Isometric view for the disc brake surface can gives a bigger picture of thermal stress distribution as shown in Figure 4.17 and 4.18 below for perforated and non perforated disc brakes. Although previous graph show that the highest thermal stress for perforated disc brake is 470.67 MPa at surface node near the inner part of the disc, isometric view show that the highest thermal stress actually occurred at the perforated hole with magnitude of 596 MPa at the end of the braking time. While the highest thermal stress value for non perforated disc is 514 MPa at the inner part of the disc at the end of the braking.

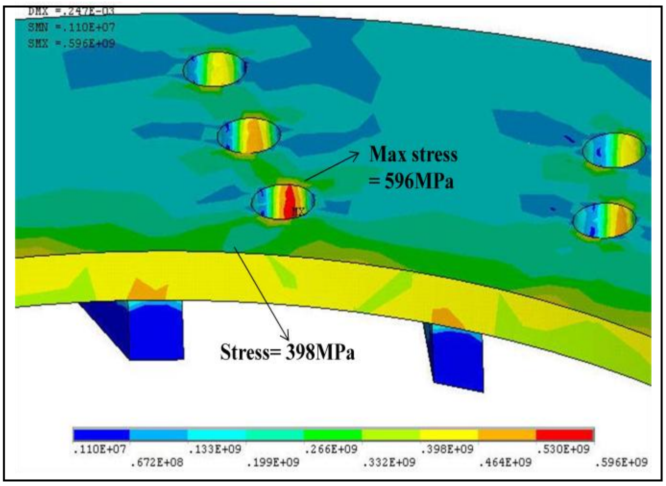

Figure 4.17: Isometric View of Perforated Disc

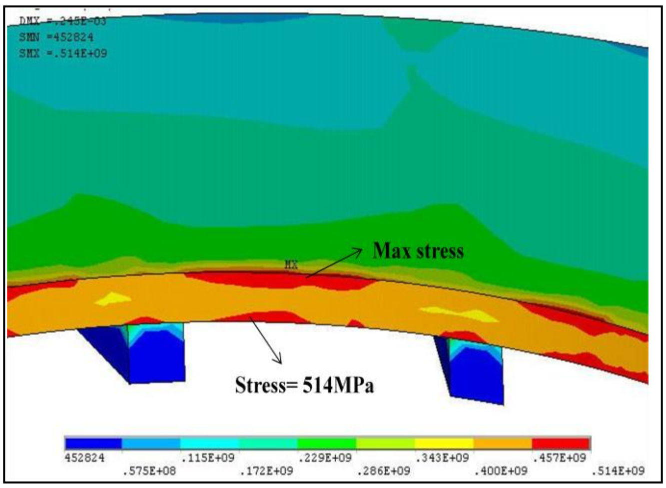

Figure 4.18: Isometric View of Non Perforated Disc

4.2.2 Thermal Stress Distribution along Frictional Surface

Thermal stress distribution can be investigated by studying its distribution along the frictional surface between disc brake and brake pad. Figure 4.19 shows the A-A' path along the radial distance of the disc brake's surface. This path is selected along the surface of solid cross section for the perforated disc brake. Thermal stress generated at different time during the simulation period is recorded in order to investigate the thermal stress distribution at these particular times. Thermal stress distribution along the frictional surface for perforated disc brake is shown in Figure 4.20 and non perforated disc brake in Figure 4.21. From both figures, the thermal stress distribution along the surface increases with the time until a maximum value at time just before the end of simulation period. This is due to the increment in the accumulated frictional heat flux to the disc brake's surface, leading to the increment of surface temperature.

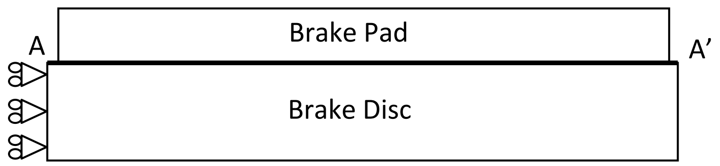

Figure 4.19: A – A' Path along the Radial Distance of Disc Brake

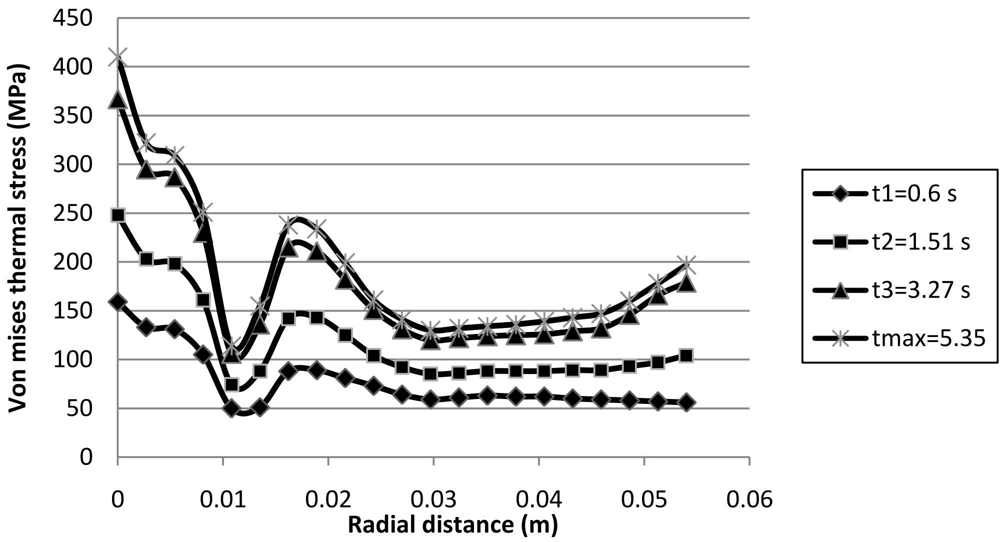

Figure 4.20: Thermal Stress Distribution along Path A – A' for Perforated Disc Brake at Different Times

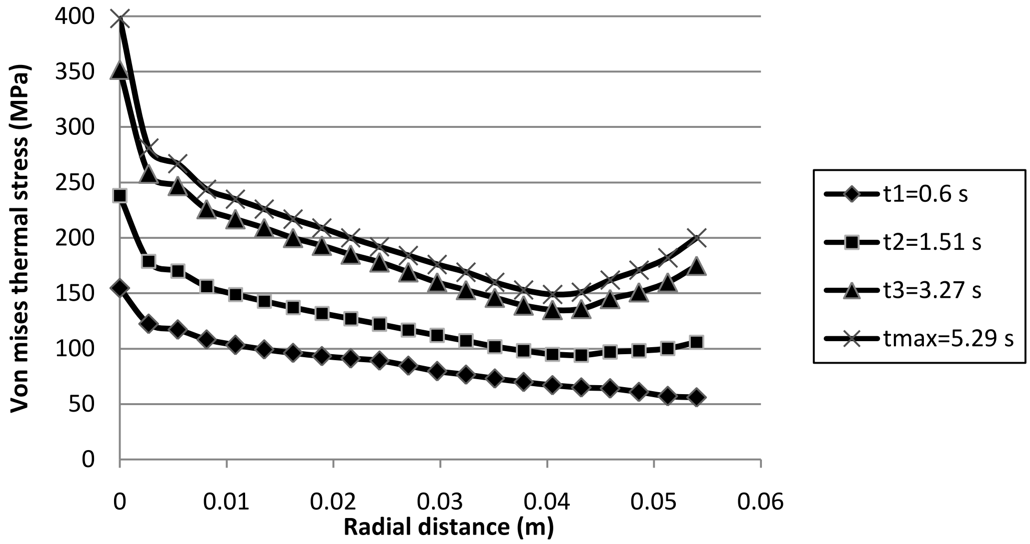

Figure 4.21: Thermal Stress Distribution along Path A – A’ for Non Perforated Disc Brake at Different Times

A more detailed thermal stress distributions are obtained by specifying path A – A’, B – B’ and C – C’ which are the paths along the disc brake’s surface, mid way along of disc brake’s thickness and along bottom of the disc brake respectively as shown in Figure 4.22. These paths are similar to the one specified for temperature distribution in Figure 4.6. Further comparison is made for both disc brakes at the time when the temperature reached its maximum for both cases, 5.35 seconds for perforated disc and 5.29 seconds for non perforated disc as shown in Figure 4.23.

The plotted thermal stress distribution curves show that the distribution patterns for all three paths have almost the same pattern for both perforated and non perforated disc. This is largely because they are all situated perpendicular to the heat source with path A – A’ received the highest magnitude of frictional heat flux at the surface followed by path B – B’ and path C – C’, which explain why the thermal stress distribution for path A – A’ is the highest, path C – C’ the lowest and path B – B’ comes in between. Through the comparison of thermal stress distribution for perforated and non perforated disc brake, it can be concluded that the perforated disc brake has a generally lower thermal stress distribution as compared to non perforated disc for all three different paths.

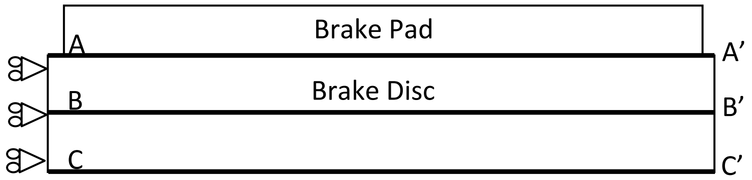

Figure 4.22: A – A’, B – B’ and C – C’ Paths along the Radial Distance of Disc Brake

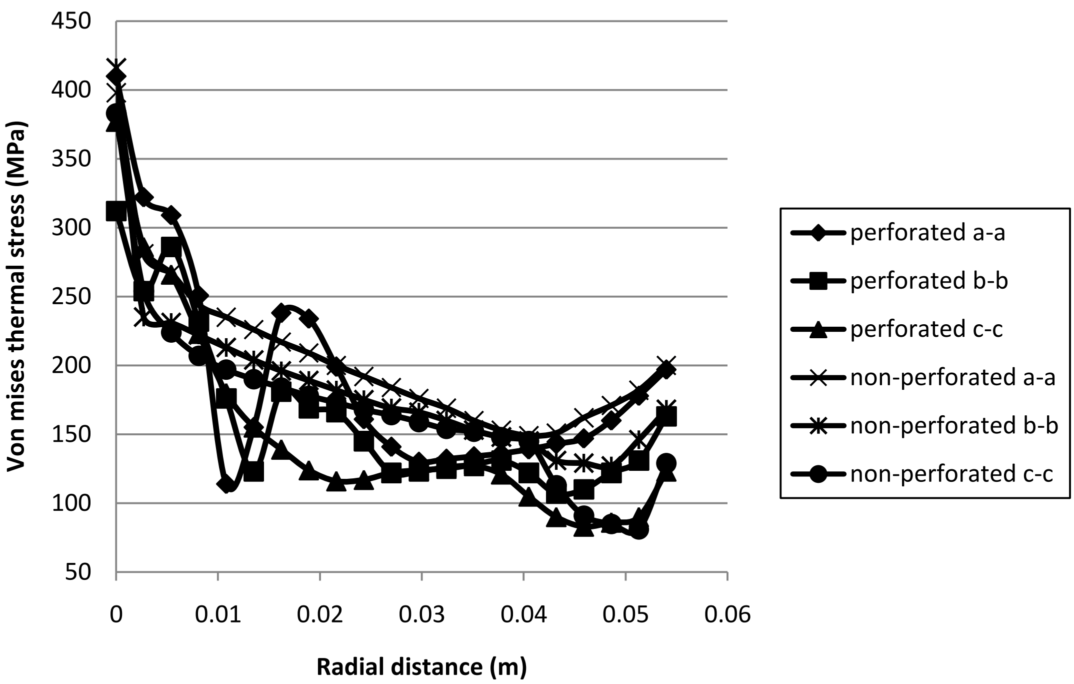

Figure 4.23: Thermal Stress Distribution along Path A-A’, B-B’ and C-C’ for Perforated and Non Perforated Disc at Time 5.35 Seconds and 5.29 Seconds Respectively

4.2.3Thermal Stress Distribution across the Cross Section

Thermal stress distribution within the disc brake body is analyzed by creating a slicing plane along the perforated holes to compare the thermal stress distribution between perforated and non perforated disc brake. Figure 4.24 and 4.25 illustrate the thermal stress distribution at the end of braking process, at 5.99 seconds.

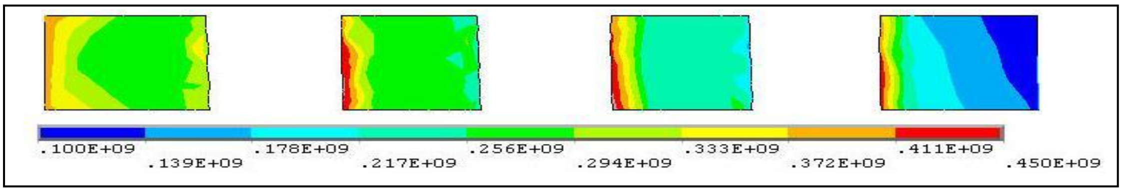

Figure 4.24: Cross Section Von Mises Stress (Perforated Disc Brake), Time 5.99s

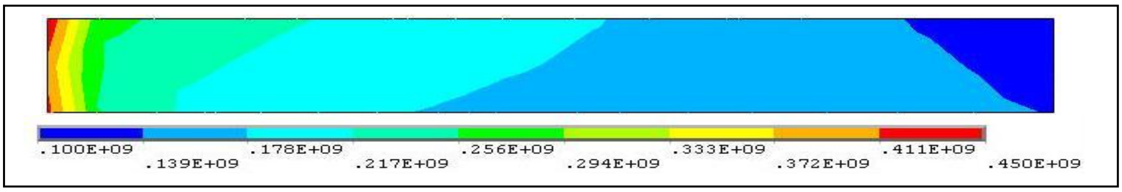

Figure 4.25: Cross Section Von Mises Stress (Non Perforated Disc Brake), Time 5.99s

Although the Von Mises stress generated at perforated disc's surface is lower than non-perforated disc brake, high magnitude of Von Mises stresses (red colored region) are generated around the perforated holes for perforated disc brake as illustrated in Figure 4.24 as compared to non perforated disc brake where high thermal stress region is situated at the inner part of the disc only. Refer to Figure 4.26 and 4.27 in Section 4.2.3.1 and 4.2.3.2 respectively for the cross section thermal stress distribution for various braking period.

4.2.3.1 Von Mises Thermal Stress Distribution across Cross Section for Perforated Disc

(a) Time= 0.51814 s

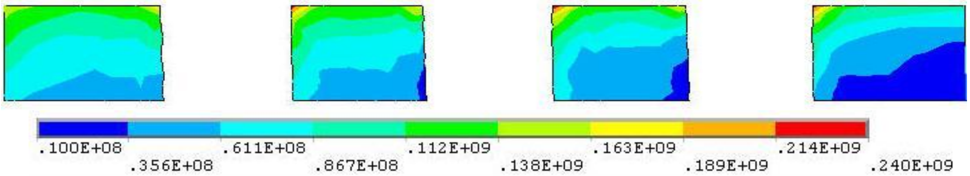

(b) Time = 1.09 s

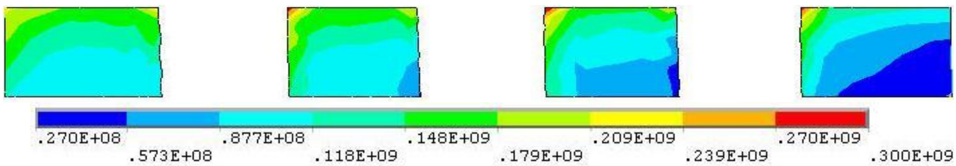

(c) Time = 1.736 s

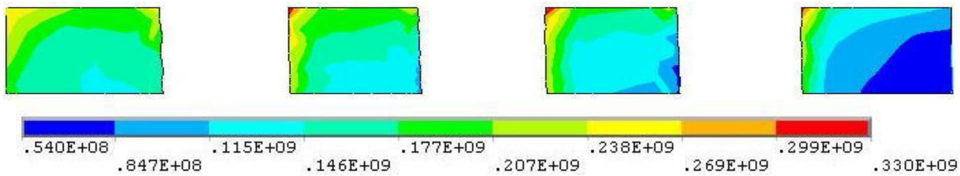

(d) Time = 2.498 s

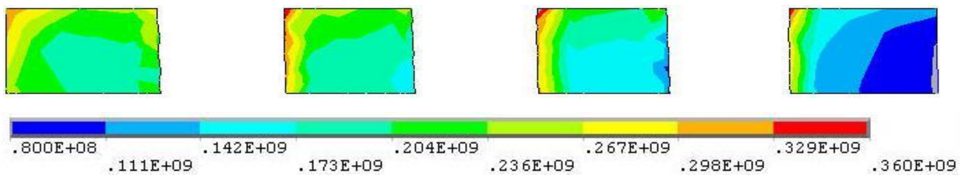

(e) Time = 4.2 s

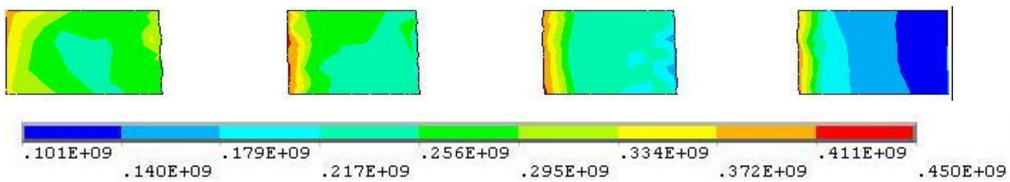

(f) Time = 5.991 s

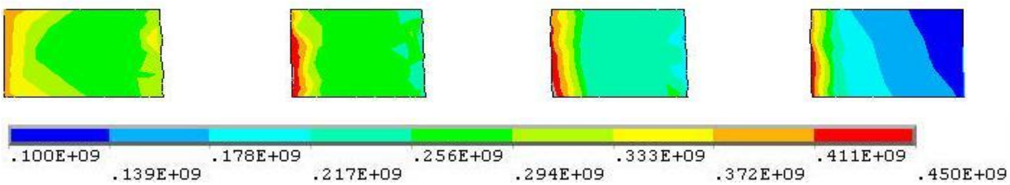

Figure 4.26: Von Mises Thermal Stress Distribution across Cross Section for Perforated Disc at Different Set of Time

4.2.3.2 Von Mises Thermal Stress Distribution across Cross Section for Non Perforated Disc

(a) Time = 0.51814 s

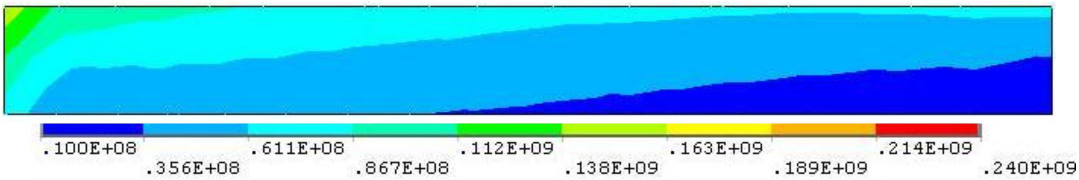

(b) Time = 1.09 s

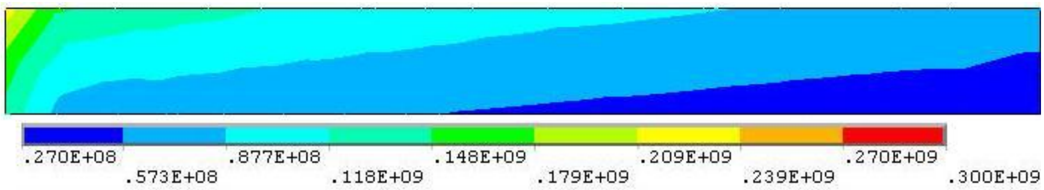

(c) Time = 1.736 s

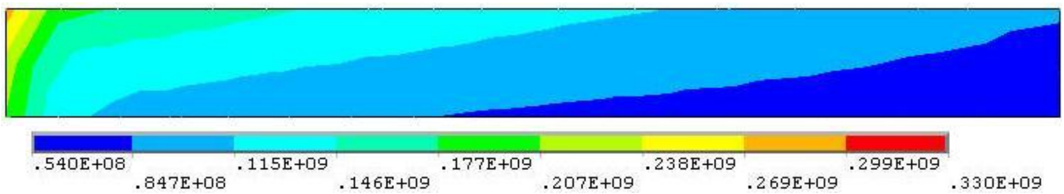

(d) Time = 2.498 s

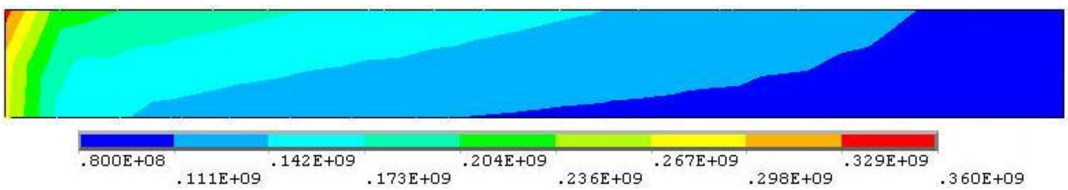

(e) Time = 4.2 s

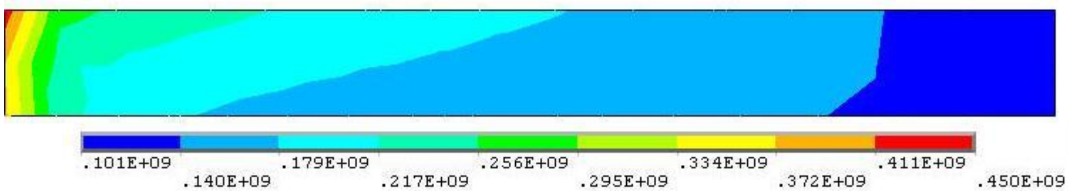

(f) Time = 5.991 s

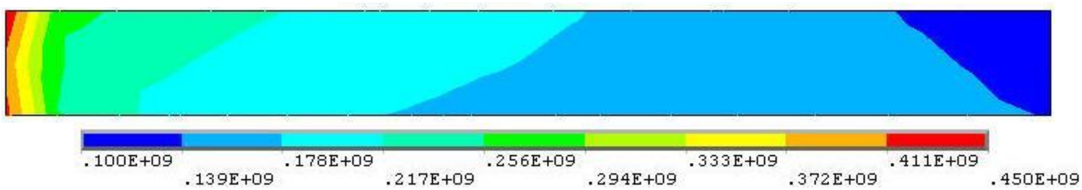

Figure 4.27: Von Mises Thermal Stress Distribution across Cross Section for Non Perforated Disc at Different Set of Time

4.2.4 Thermal Stress Contour

Another interesting observation is the surface's thermal stress distribution of the whole disc brake. It gives a bigger picture of the effects of perforation on the thermal stress distribution. Figure 4.28 below shows the top surface's thermal stress distribution at time 5.99 seconds. Refer to Appendix F for thermal stress distribution (disc brake's top view) in various braking period.

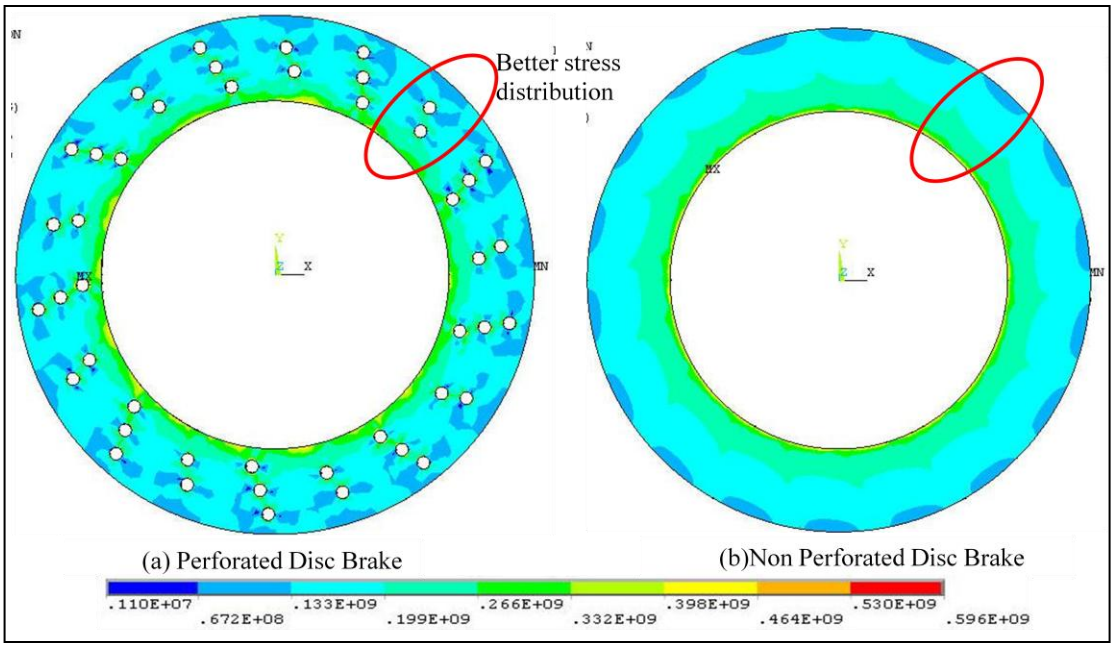

Figure 4.28: Top Surface Thermal Stress Distribution, Time 5.99s

The overall top surface thermal stress distribution shows that the perforated disc brake has better stress distribution with more distribution of lower stress region (blue colored) over the whole surface as compared to non perforated disc brake. This observation is also true for the bottom surface of both disc brakes where perforated disc brake also has better stress distribution with more distribution of lower stress region (blue colored) as shown in Figure 4.29.

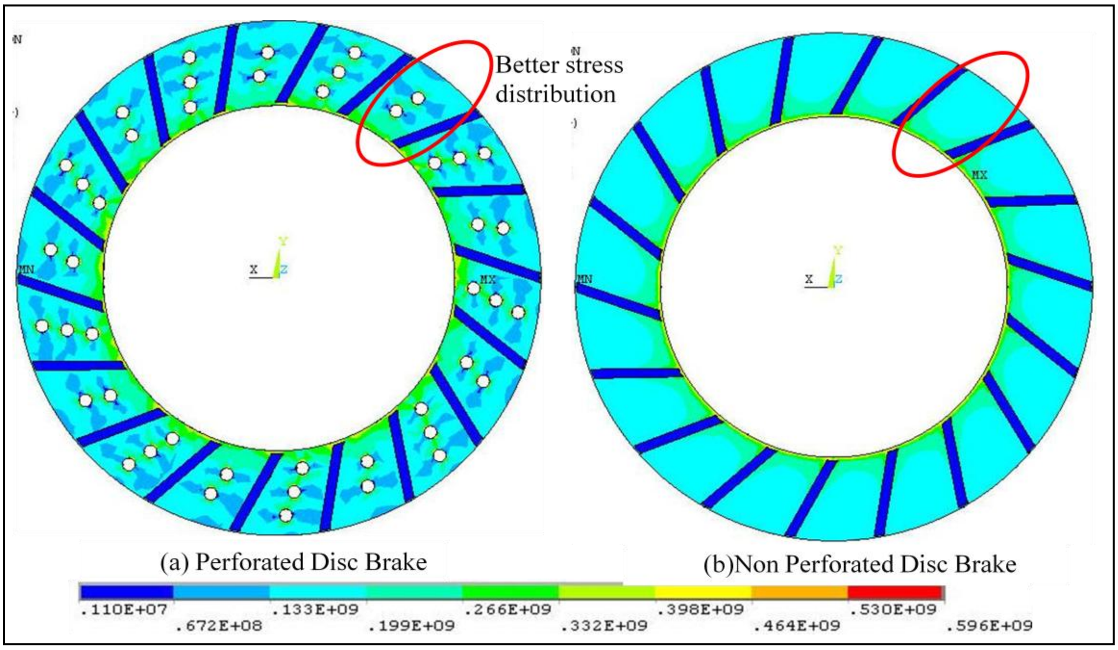

Figure 4.29: Bottom Surface Thermal Stress Distribution, Time 5.99s

CHAPTER 5
CONCLUSION AND RECOMMENDATIONS

This project is critical and practical in analyzing the thermal stresses that arise from the high temperature distribution along the perforated brake disc surface, where the perforated holes are often referred to as the stress concentration zones that will contribute to the cracking of the disc in the end of severe usage. This phenomenon is confirmed through the simulation performed on the perforated disc brake in this project where the results clearly showed highly concentrated thermal stress exists around the area of perforated hole's circumference. On the other hand, another interesting area of analysis in this project is to investigate the effects of the perforated holes to the overall performance of the disc brake. This is done by comparing the overall thermal stress distribution between perforated and non perforated disc brake where the results show that the perforated disc brake has a better thermal stress distribution over the surface and body as compared to non perforated disc brake in general. Conclusion can draw that the perforated disc brake is better in increasing the performance of the vehicle but the weighting are between the high stress concentration at the perforated zones and better cooling ability of the perforated brake disc in comparison to the conventional disc brake.

There are three recommendations for future work expansion related to perforated disc brake which can be carry out to further understand the effects of having perforated holes under various designs. The recommendations are as following:

1. Analyze the effects of different perforated holes patterns on disc brake's temperature and thermal stress distributions.
2. Analyze the effects of different density of perforated holes on disc brake's temperature and thermal stress distributions.
3. Analyze the effects of different disc brake's materials on its temperature and thermal stress distributions, such as cast iron, reinforced carbon-carbon and ceramic matrix composites.

REFERENCES

1. Wikipedia. 24 July 2009 < http://en.wikipedia.org/wiki/Disc_brake>.

2. howstuffworks.com, <http://auto.howstuffworks.com/auto-parts/brakes/brake-types/disc-brake.htm/printable>.

3. Ji-Hoon Choi and In Lee, 2004, "Finite element analysis of transient thermoelastic behaviors in disk brakes", Elsevier B.V., Wear, Volume 257 (issues 1-2), Pages 47- 58.

4. Christopher J Longhurst. 3 August 2009 <http://www.carbibles.com/brake_bible.html>.

5. Mohd Adam Bin Omar. 2009, Thermal Stress Distribution In Brake Disc For Small Vehicle, Final Year Project, Bachelor of Engineering (Hons), Universiti Teknologi PETRONAS, Malaysia.

6. Robert W. Soutas-Little, 1999, "Elasticity", New York, Dover Publications.

7. D.J. Kim, Y.M. Lee, J.S. Park and C.S. Seok, 2008, "Thermal stress analysis for a disc brake of railway vehicles with the consideration of the pressure distribution on a frictional surface", Elsevier B.V., Materials Science and Engineering, Volume 483-484, Pages 456-459.

8. Thomas J. Mackin and group, 2002, "Thermal cracking in disc brakes", Elsevier B.V., Engineering Failure Analysis, Volume 9 (Issue 1), Pages 63-76.

9. Wikipedia. 23 October 2009 <http://en.wikipedia.org/wiki/Finite_element_method>

10. C.H. Gao and X.Z. Lin, 2002, " Transient temperature field analysis of a brake in a non-axisymmetric three dimensional model", Elsevier B.V., Journal of Material Processing Technology.

11. M. Elthoukhy, S. Asfour, M. Almakky, C. Huang, 2006, “ Thermoelastic instability in disc brakes: Simulation of the heat generation problem”, Department of industrial engineering, University of Miami, Department of production engineering, Alexandria University, Department of biomedical engineering, University of Miami.

12. Akio Sonoda, Suguru Kashiwagi, Shigeru Hamada and Hiroshi Noguchi, 2008, “Quantitative evaluation of heat crack initiation condition under thermal shock”, Journal of Solid Mechanics and Materials Engineering, Volume 2, No.1, Pages 128-136.

13. Faruk Sen and Kemal Aldas, 2009, “Elastic-plastic themal stress analysis in a thermalplastic composite disc applied linear temperature loads via FEM”, Elsevier B.V., Advances in Engineering Software, Volume 40 (Issue 9), Pages 813-819.

14. Pier Francesco Gotowicki, Prof. Vinzenco Nigrelli, Prof. Gabriele Virzi Mariotti, Mgr. Dipl. Ing. Dragan Aleksendric, Prof. Dr. Cedom ir Duboka, 2005, “ Numerical and experimental analysis of a pegswing ventilated disk brake rotor, with pads and cylinders”, BEOGRAD 2005 EAEC European Automotive Congress.

Appendix A. Vehicle Specifications

1) Engine capacity: 2.4 liter (2400 cc)
2) Vehicle weight: 1465kg
3) Maximum car weight: 1950kg
   a) Front gross axle weight rating: 1060kg
   b) Rear gross axle weight rating: 915kg
4) Weight ratio:
   a) Front ratio = $\frac{1060kg}{1950kg}$ = 0.54
   b) Rear ratio = $\frac{915kg}{1950kg}$ = 0.46
5) Considering maximum car weight for further analysis:

   Car weight = 1950kg
   a) Front wheel applied weight = 1950kg * front weight ratio

      = 1950kg * 0.54 ≈ 1053kg
   b) Rear wheel applied weight = 1950kg * rear weight ratio

      = 1950kg * 0.46 ≈ 897kg
6) Weight applied on each disc brake surface
   a) By taking the weight on a more severe/higher weight side of the vehicle, attention is focused to the front wheel applied weight of 1053kg.
   b) There are two brakes at the left and right hand side of the front wheel where the applied weight is equally distributed:

      Weight on one side of the front wheel = $\frac{1053kg}{2}$ = 526.5 kg
   c) For thermal stress analysis purpose, only one side of the disc brake will be considered. (Asymmetrical analysis). Thus, the weight on each disc brake surface:

      Weight on each disc brake surface = $\frac{526.5kg}{2}$ = 263.25 kg

Appendix B. Disc Brake Kinetic Calculation

1) Time taken to stop vehicle:

$t = \frac{v-u}{a}$

u = 150 km/hr = 41.67m/s

v = 0 m/s

a = -0.7 Gravity = - 6.867 m/s^2

$t = \frac{0-41.67\ m/s}{-\ 6.867\ m/s^2}$

= 6.068 s

2) Distance travelled before stopping:

$v^2 = u^2 + 2\ as$

$s = \frac{1}{2a}\,(v^2 - u^2)$

$= \frac{1}{2(-6.867)}\,(0 - (41.67^2))$

= 126.43 m

3) Pad contact area:

Perimeter of disc brake = $2\pi r_{disc}$

= 2π (0.164 m)

= 1.030 m

Length of pad = 0.186 m

Degree of covered area = $\frac{0.186\ m}{1.030\ m}$ x 360 º

= 65 º

For simplification of analysis, we take the covered area as 60º

Thus, pad contact area = $[(\pi {r_{out}}^2) - (\pi {r_{in}}^2)] \times \frac{60°}{360°}$

$= [(\pi 0.164^2) - (\pi 0.11^2)] \times \frac{60°}{360°}$

= 0.00775 m^2

4) Disc initial angular velocity:

$\omega_{tire} = \omega_{disc}$

$v_{tire} = r_{tire}\omega_{tire}$

$41.67\text{m/s} = \frac{0.658\ m}{2}\ \omega_{tire}$

ω_{tire}= <u>126.66 rad/s</u>

And, $v_{disc} = r_{disc}\omega_{disc}$

$= \frac{0.328\ m}{2}\ (126.66)$

= <u>20.77 m/s</u>

5) Disc initial angular acceleration

$\alpha_{tire} = \alpha_{disc}$

$a_{tire} = r_{tire}\alpha_{tire}$

$-6.867\text{m}/s^2 = \frac{0.658\ m}{2}\ \alpha_{tire}$

α_{tire} = <u>-20.87 rad/s^2</u>

And, $a_{disc} = r_{disc}\alpha_{disc}$

$= \frac{0.328\ m}{2}\ (-20.87)$

= <u>- 3.423 m/s^2</u>

6) Initial angular velocity of next pad rotational:

$\omega_j^2 = \omega_i^2 + 2\ \alpha\ \theta$

$\theta = \frac{S}{r} = \frac{2\ \pi\ (0.164\text{m})\ \text{x}\ \frac{60°}{360°}}{0.164\ m}$

= 1.0471

$\omega_j = [(126.66^2) + 2(-20.87)\ (1.0471)]^{1/2}$

= <u>126.48 rad/s</u>

7) Time interval between 2 pad rotational positions:

$\omega_j = \omega_i + \alpha\ t$

$\Delta\ t = \frac{\omega_j - \omega_i}{\alpha}$

$= \frac{126.48 - 126.66}{-20.87}$

= <u>0.00862 s</u>

8) Heat energy absorbed by the disc brake:

- 95 % of heat absorbed by disc and 5% by pad
- Load, m = 263.25 kg
- v_i = 41.67 m/s
- $v_j = r_{tire}\omega_j$

  = 0.329 m x 126.48 rad/s

  = 41.612 m/s

ΔQ = 0.95 (Kinetic energy)

$= 0.95 [\frac{1}{2} \times m \times (v_i^2 - v_j^2)]$

$= 0.95 [\frac{1}{2} \times 263.25 \times (41.67^2 - 41.612^2)]$

= <u>604.0 Joule</u>

9) Heat flux at contact area (heat transfer per unit area):

Heat flux, $\dot{q} = \frac{\dot{Q}}{A} = \frac{\Delta Q}{A\,t}$

$= \frac{604.0\ J}{0.00862\ (0.00775\ m^2)}$

= <u>9.041 MW/m^2</u>

Appendix C. Disc Brake Kinetic Calculations

No. of pad rotational	Time interval (s)	Total time (s)	Angular velocity (rad/s)	Velocity (m/s)	Heat absorbed by disc (J)	Accumulative heat (J)	Heat flux (W/m2)
0	0	0	126.660	41.671	0	0	0
1	0.00827	0.00827	126.487	41.614	591.6105	591.6105	9226731.626
2	0.00828	0.01656	126.314	41.557	591.6105	1183.2210	9214136.284
3	0.00830	0.02485	126.141	41.500	591.6105	1774.8315	9201523.7
4	0.00831	0.03316	125.968	41.443	591.6105	2366.4419	9188893.805
5	0.00832	0.04148	125.794	41.386	591.6105	2958.0524	9176246.526
6	0.00833	0.04981	125.620	41.329	591.6105	3549.6629	9163581.792
7	0.00834	0.05815	125.446	41.272	591.6105	4141.2734	9150899.53
8	0.00835	0.06651	125.272	41.214	591.6105	4732.8839	9138199.668
9	0.00837	0.07487	125.097	41.157	591.6105	5324.4944	9125482.131
10	0.00838	0.08325	124.923	41.100	591.6105	5916.1049	9112746.845
11	0.00839	0.09164	124.748	41.042	591.6105	6507.7154	9099993.737
12	0.00840	0.10004	124.572	40.984	591.6105	7099.3258	9087222.731
13	0.00841	0.10845	124.397	40.926	591.6105	7690.9363	9074433.751
14	0.00842	0.11687	124.221	40.869	591.6105	8282.5468	9061626.722
15	0.00844	0.12531	124.045	40.811	591.6105	8874.1573	9048801.567
16	0.00845	0.13376	123.868	40.753	591.6105	9465.7678	9035958.208
17	0.00846	0.14222	123.692	40.695	591.6105	10057.3783	9023096.569
18	0.00847	0.15069	123.515	40.636	591.6105	10648.9888	9010216.57
19	0.00848	0.15918	123.338	40.578	591.6105	11240.5992	8997318.132
20	0.00850	0.16767	123.161	40.520	591.6105	11832.2097	8984401.178
21	0.00851	0.17618	122.983	40.461	591.6105	12423.8202	8971465.625
22	0.00852	0.18470	122.805	40.403	591.6105	13015.4307	8958511.394
23	0.00853	0.19324	122.627	40.344	591.6105	13607.0412	8945538.404
24	0.00855	0.20178	122.449	40.286	591.6105	14198.6517	8932546.573
25	0.00856	0.21034	122.270	40.227	591.6105	14790.2622	8919535.819
26	0.00857	0.21891	122.091	40.168	591.6105	15381.8727	8906506.058
27	0.00858	0.22749	121.912	40.109	591.6105	15973.4831	8893457.207
28	0.00860	0.23609	121.733	40.050	591.6105	16565.0936	8880389.183
29	0.00861	0.24470	121.553	39.991	591.6105	17156.7041	8867301.899
30	0.00862	0.25332	121.373	39.932	591.6105	17748.3146	8854195.272
31	0.00863	0.26196	121.193	39.872	591.6105	18339.9251	8841069.214
32	0.00865	0.27060	121.013	39.813	591.6105	18931.5356	8827923.639
33	0.00866	0.27926	120.832	39.754	591.6105	19523.1461	8814758.46
34	0.00867	0.28794	120.651	39.694	591.6105	20114.7566	8801573.589
35	0.00869	0.29662	120.470	39.634	591.6105	20706.3670	8788368.937
36	0.00870	0.27926	120.288	39.575	591.6105	19523.1461	8775144.415
37	0.00871	0.31403	120.106	39.515	591.6105	21889.5880	8761899.933
38	0.00873	0.32276	119.924	39.455	591.6105	22481.1985	8748635.4

39	0.00874	0.33150	119.742	39.395	591.6105	23072.8090	8735350.725
40	0.00875	0.34025	119.559	39.335	591.6105	23664.4195	8722045.816
41	0.00877	0.34902	119.376	39.275	591.6105	24256.0300	8708720.58
42	0.00878	0.35779	119.193	39.214	591.6105	24847.6404	8695374.924
43	0.00879	0.36659	119.009	39.154	591.6105	25439.2509	8682008.753
44	0.00881	0.37539	118.826	39.094	591.6105	26030.8614	8668621.973
45	0.00882	0.38421	118.641	39.033	591.6105	26622.4719	8655214.488
46	0.00883	0.39305	118.457	38.972	591.6105	27214.0824	8641786.202
47	0.00885	0.40189	118.272	38.912	591.6105	27805.6929	8628337.017
48	0.00886	0.41075	118.088	38.851	591.6105	28397.3034	8614866.836
49	0.00887	0.41963	117.902	38.790	591.6105	28988.9139	8601375.56
50	0.00889	0.42852	117.717	38.729	591.6105	29580.5243	8587863.09
51	0.00890	0.43742	117.531	38.668	591.6105	30172.1348	8574329.324
52	0.00892	0.44634	117.345	38.606	591.6105	30763.7453	8560774.164
53	0.00893	0.45527	117.159	38.545	591.6105	31355.3558	8547197.505
54	0.00895	0.46422	116.972	38.484	591.6105	31946.9663	8533599.247
55	0.00896	0.47317	116.785	38.422	591.6105	32538.5768	8519979.286
56	0.00897	0.48215	116.598	38.361	591.6105	33130.1873	8506337.516
57	0.00899	0.49114	116.410	38.299	591.6105	33721.7977	8492673.834
58	0.00900	0.50014	116.222	38.237	591.6105	34313.4082	8478988.133
59	0.00902	0.50916	116.034	38.175	591.6105	34905.0187	8465280.307
60	0.00903	0.51819	115.845	38.113	591.6105	35496.6292	8451550.247
61	0.00905	0.52724	115.657	38.051	591.6105	36088.2397	8437797.846
62	0.00906	0.53630	115.467	37.989	591.6105	36679.8502	8424022.994
63	0.00908	0.54538	115.278	37.926	591.6105	37271.4607	8410225.58
64	0.00909	0.55447	115.088	37.864	591.6105	37863.0712	8396405.493
65	0.00911	0.56357	114.898	37.802	591.6105	38454.6816	8382562.622
66	0.00912	0.57270	114.708	37.739	591.6105	39046.2921	8368696.853
67	0.00914	0.58183	114.517	37.676	591.6105	39637.9026	8354808.072
68	0.00915	0.59099	114.326	37.613	591.6105	40229.5131	8340896.164
69	0.00917	0.60015	114.135	37.550	591.6105	40821.1236	8326961.014
70	0.00918	0.60934	113.943	37.487	591.6105	41412.7341	8313002.503
71	0.00920	0.61853	113.751	37.424	591.6105	42004.3446	8299020.516
72	0.00921	0.62775	113.559	37.361	591.6105	42595.9551	8285014.931
73	0.00923	0.63698	113.366	37.298	591.6105	43187.5655	8270985.631
74	0.00925	0.64622	113.173	37.234	591.6105	43779.1760	8256932.494
75	0.00926	0.65548	112.980	37.170	591.6105	44370.7865	8242855.397
76	0.00928	0.66476	112.786	37.107	591.6105	44962.3970	8228754.219
77	0.00929	0.67405	112.593	37.043	591.6105	45554.0075	8214628.834
78	0.00931	0.68336	112.398	36.979	591.6105	46145.6180	8200479.118
79	0.00932	0.69269	112.204	36.915	591.6105	46737.2285	8186304.945
80	0.00934	0.70203	112.009	36.851	591.6105	47328.8389	8172106.188
81	0.00936	0.71139	111.813	36.787	591.6105	47920.4494	8157882.718
82	0.00937	0.72076	111.618	36.722	591.6105	48512.0599	8143634.405
83	0.00939	0.73015	111.422	36.658	591.6105	49103.6704	8129361.119

84	0.00941	0.73956	111.225	36.593	591.6105	49695.2809	8115062.728
85	0.00942	0.74898	111.029	36.528	591.6105	50286.8914	8100739.1
86	0.00944	0.75842	110.832	36.464	591.6105	50878.5019	8086390.1
87	0.00946	0.76788	110.634	36.399	591.6105	51470.1124	8072015.592
88	0.00947	0.77735	110.437	36.334	591.6105	52061.7228	8057615.441
89	0.00949	0.78684	110.239	36.269	591.6105	52653.3333	8043189.509
90	0.00951	0.79635	110.040	36.203	591.6105	53244.9438	8028737.656
91	0.00953	0.80587	109.841	36.138	591.6105	53836.5543	8014259.743
92	0.00954	0.81542	109.642	36.072	591.6105	54428.1648	7999755.627
93	0.00956	0.82498	109.443	36.007	591.6105	55019.7753	7985225.167
94	0.00958	0.83455	109.243	35.941	591.6105	55611.3858	7970668.218
95	0.00959	0.84415	109.043	35.875	591.6105	56202.9962	7956084.634
96	0.00961	0.85376	108.842	35.809	591.6105	56794.6067	7941474.269
97	0.00963	0.86339	108.641	35.743	591.6105	57386.2172	7926836.975
98	0.00965	0.87304	108.440	35.677	591.6105	57977.8277	7912172.603
99	0.00967	0.88271	108.238	35.610	591.6105	58569.4382	7897481.001
100	0.00968	0.89239	108.036	35.544	591.6105	59161.0487	7882762.017
101	0.00970	0.90209	107.833	35.477	591.6105	59752.6592	7868015.498
102	0.00972	0.91181	107.630	35.410	591.6105	60344.2697	7853241.289
103	0.00974	0.92155	107.427	35.344	591.6105	60935.8801	7838439.232
104	0.00976	0.93131	107.224	35.277	591.6105	61527.4906	7823609.17
105	0.00978	0.94108	107.020	35.209	591.6105	62119.1011	7808750.944
106	0.00979	0.95088	106.815	35.142	591.6105	62710.7116	7793864.391
107	0.00981	0.96069	106.610	35.075	591.6105	63302.3221	7778949.351
108	0.00983	0.97052	106.405	35.007	591.6105	63893.9326	7764005.657
109	0.00985	0.98037	106.200	34.940	591.6105	64485.5431	7749033.146
110	0.00987	0.99024	105.994	34.872	591.6105	65077.1536	7734031.648
111	0.00989	1.00013	105.787	34.804	591.6105	65668.7640	7719000.996
112	0.00991	1.01004	105.580	34.736	591.6105	66260.3745	7703941.019
113	0.00993	1.01997	105.373	34.668	591.6105	66851.9850	7688851.544
114	0.00995	1.02992	105.166	34.599	591.6105	67443.5955	7673732.397
115	0.00997	1.03989	104.958	34.531	591.6105	68035.2060	7658583.402
116	0.00999	1.04987	104.749	34.462	591.6105	68626.8165	7643404.383
117	0.01001	1.05988	104.540	34.394	591.6105	69218.4270	7628195.16
118	0.01003	1.06991	104.331	34.325	591.6105	69810.0374	7612955.551
119	0.01005	1.07996	104.121	34.256	591.6105	70401.6479	7597685.375
120	0.01007	1.09002	103.911	34.187	591.6105	70993.2584	7582384.446
121	0.01009	1.10011	103.701	34.118	591.6105	71584.8689	7567052.577
122	0.01011	1.11022	103.490	34.048	591.6105	72176.4794	7551689.581
123	0.01013	1.12035	103.278	33.979	591.6105	72768.0899	7536295.267
124	0.01015	1.13050	103.066	33.909	591.6105	73359.7004	7520869.442
125	0.01017	1.14067	102.854	33.839	591.6105	73951.3109	7505411.913
126	0.01019	1.15086	102.642	33.769	591.6105	74542.9213	7489922.483
127	0.01021	1.16108	102.428	33.699	591.6105	75134.5318	7474400.953

128	0.01023	1.17131	102.215	33.629	591.6105	75726.1423	7458847.124
129	0.01026	1.18157	102.001	33.558	591.6105	76317.7528	7443260.793
130	0.01028	1.19184	101.786	33.488	591.6105	76909.3633	7427641.755
131	0.01030	1.20214	101.571	33.417	591.6105	77500.9738	7411989.803
132	0.01032	1.21246	101.356	33.346	591.6105	78092.5843	7396304.729
133	0.01034	1.22281	101.140	33.275	591.6105	78684.1947	7380586.321
134	0.01037	1.23317	100.924	33.204	591.6105	79275.8052	7364834.366
135	0.01039	1.24356	100.707	33.133	591.6105	79867.4157	7349048.648
136	0.01041	1.25397	100.490	33.061	591.6105	80459.0262	7333228.95
137	0.01043	1.26440	100.272	32.989	591.6105	81050.6367	7317375.05
138	0.01045	1.27486	100.054	32.918	591.6105	81642.2472	7301486.726
139	0.01048	1.28533	99.835	32.846	591.6105	82233.8577	7285563.753
140	0.01050	1.29583	99.616	32.774	591.6105	82825.4682	7269605.902
141	0.01052	1.30636	99.396	32.701	591.6105	83417.0786	7253612.945
142	0.01055	1.31690	99.176	32.629	591.6105	84008.6891	7237584.648
143	0.01057	1.32748	98.956	32.556	591.6105	84600.2996	7221520.775
144	0.01059	1.33807	98.734	32.484	591.6105	85191.9101	7205421.09
145	0.01062	1.34869	98.513	32.411	591.6105	85783.5206	7189285.351
146	0.01064	1.35933	98.291	32.338	591.6105	86375.1311	7173113.314
147	0.01067	1.37000	98.068	32.264	591.6105	86966.7416	7156904.735
148	0.01069	1.38069	97.845	32.191	591.6105	87558.3521	7140659.364
149	0.01071	1.39140	97.621	32.117	591.6105	88149.9625	7124376.949
150	0.01074	1.40214	97.397	32.044	591.6105	88741.5730	7108057.236
151	0.01076	1.41291	97.173	31.970	591.6105	89333.1835	7091699.967
152	0.01079	1.42369	96.947	31.896	591.6105	89924.7940	7075304.882
153	0.01081	1.43451	96.722	31.821	591.6105	90516.4045	7058871.717
154	0.01084	1.44535	96.496	31.747	591.6105	91108.0150	7042400.206
155	0.01087	1.45621	96.269	31.672	591.6105	91699.6255	7025890.079
156	0.01089	1.46710	96.042	31.598	591.6105	92291.2359	7009341.064
157	0.01092	1.47802	95.814	31.523	591.6105	92882.8464	6992752.883
158	0.01094	1.48896	95.585	31.448	591.6105	93474.4569	6976125.258
159	0.01097	1.49993	95.356	31.372	591.6105	94066.0674	6959457.906
160	0.01100	1.51093	95.127	31.297	591.6105	94657.6779	6942750.541
161	0.01102	1.52195	94.897	31.221	591.6105	95249.2884	6926002.873
162	0.01105	1.53300	94.666	31.145	591.6105	95840.8989	6909214.609
163	0.01108	1.54407	94.435	31.069	591.6105	96432.5094	6892385.453
164	0.01110	1.55518	94.203	30.993	591.6105	97024.1198	6875515.104
165	0.01113	1.56631	93.971	30.917	591.6105	97615.7303	6858603.259
166	0.01116	1.57746	93.738	30.840	591.6105	98207.3408	6841649.609
167	0.01119	1.58865	93.505	30.763	591.6105	98798.9513	6824653.843
168	0.01121	1.59986	93.271	30.686	591.6105	99390.5618	6807615.645
169	0.01124	1.61110	93.036	30.609	591.6105	99982.1723	6790534.697
170	0.01127	1.62237	92.801	30.532	591.6105	100573.7828	6773410.674
171	0.01130	1.63367	92.565	30.454	591.6105	101165.3932	6756243.249

172	0.01133	1.64500	92.329	30.376	591.6105	101757.0037	6739032.092
173	0.01136	1.65636	92.092	30.298	591.6105	102348.6142	6721776.864
174	0.01139	1.66774	91.854	30.220	591.6105	102940.2247	6704477.227
175	0.01142	1.67916	91.616	30.142	591.6105	103531.8352	6687132.836
176	0.01145	1.69060	91.377	30.063	591.6105	104123.4457	6669743.341
177	0.01148	1.70208	91.138	29.984	591.6105	104715.0562	6652308.388
178	0.01151	1.71358	90.897	29.905	591.6105	105306.6667	6634827.621
179	0.01154	1.72512	90.657	29.826	591.6105	105898.2771	6617300.674
180	0.01157	1.73669	90.415	29.747	591.6105	106489.8876	6599727.181
181	0.01160	1.74829	90.173	29.667	591.6105	107081.4981	6582106.768
182	0.01163	1.75991	89.931	29.587	591.6105	107673.1086	6564439.059
183	0.01166	1.77157	89.687	29.507	591.6105	108264.7191	6546723.668
184	0.01169	1.78327	89.443	29.427	591.6105	108856.3296	6528960.21
185	0.01172	1.79499	89.199	29.346	591.6105	109447.9401	6511148.29
186	0.01176	1.80675	88.953	29.266	591.6105	110039.5506	6493287.509
187	0.01179	1.81854	88.707	29.185	591.6105	110631.1610	6475377.464
188	0.01182	1.83036	88.460	29.103	591.6105	111222.7715	6457417.743
189	0.01185	1.84221	88.213	29.022	591.6105	111814.3820	6439407.933
190	0.01189	1.85410	87.965	28.940	591.6105	112405.9925	6421347.61
191	0.01192	1.86602	87.716	28.859	591.6105	112997.6030	6403236.348
192	0.01196	1.87798	87.467	28.777	591.6105	113589.2135	6385073.713
193	0.01199	1.88997	87.216	28.694	591.6105	114180.8240	6366859.266
194	0.01202	1.90199	86.965	28.612	591.6105	114772.4344	6348592.56
195	0.01206	1.91405	86.714	28.529	591.6105	115364.0449	6330273.143
196	0.01209	1.92614	86.461	28.446	591.6105	115955.6554	6311900.557
197	0.01213	1.93827	86.208	28.363	591.6105	116547.2659	6293474.335
198	0.01217	1.95044	85.954	28.279	591.6105	117138.8764	6274994.005
199	0.01220	1.96264	85.700	28.195	591.6105	117730.4869	6256459.088
200	0.01224	1.97488	85.444	28.111	591.6105	118322.0974	6237869.097
201	0.01227	1.98715	85.188	28.027	591.6105	118913.7079	6219223.538
202	0.01231	1.99946	84.931	27.942	591.6105	119505.3183	6200521.909
203	0.01235	2.01181	84.673	27.858	591.6105	120096.9288	6181763.703
204	0.01239	2.02420	84.415	27.773	591.6105	120688.5393	6162948.401
205	0.01242	2.03662	84.156	27.687	591.6105	121280.1498	6144075.481
206	0.01246	2.04909	83.896	27.602	591.6105	121871.7603	6125144.408
207	0.01250	2.06159	83.635	27.516	591.6105	122463.3708	6106154.643
208	0.01254	2.07413	83.373	27.430	591.6105	123054.9813	6087105.636
209	0.01258	2.08671	83.110	27.343	591.6105	123646.5917	6067996.828
210	0.01262	2.09933	82.847	27.257	591.6105	124238.2022	6048827.654
211	0.01266	2.11199	82.583	27.170	591.6105	124829.8127	6029597.538
212	0.01270	2.12469	82.318	27.083	591.6105	125421.4232	6010305.893
213	0.01274	2.13743	82.052	26.995	591.6105	126013.0337	5990952.127
214	0.01278	2.15022	81.785	26.907	591.6105	126604.6442	5971535.635
215	0.01283	2.16304	81.517	26.819	591.6105	127196.2547	5952055.803

216	0.01287	2.17591	81.249	26.731	591.6105	127787.8652	5932512.007
217	0.01291	2.18882	80.979	26.642	591.6105	128379.4756	5912903.614
218	0.01295	2.20177	80.709	26.553	591.6105	128971.0861	5893229.977
219	0.01300	2.21477	80.438	26.464	591.6105	129562.6966	5873490.442
220	0.01304	2.22781	80.166	26.374	591.6105	130154.3071	5853684.341
221	0.01309	2.24089	79.893	26.285	591.6105	130745.9176	5833810.998
222	0.01313	2.25402	79.619	26.194	591.6105	131337.5281	5813869.722
223	0.01318	2.26720	79.344	26.104	591.6105	131929.1386	5793859.811
224	0.01322	2.28042	79.068	26.013	591.6105	132520.7490	5773780.553
225	0.01327	2.29369	78.791	25.922	591.6105	133112.3595	5753631.221
226	0.01331	2.30700	78.513	25.831	591.6105	133703.9700	5733411.076
227	0.01336	2.32036	78.234	25.739	591.6105	134295.5805	5713119.367
228	0.01341	2.33377	77.954	25.647	591.6105	134887.1910	5692755.328
229	0.01346	2.34723	77.673	25.555	591.6105	135478.8015	5672318.18
230	0.01351	2.36074	77.391	25.462	591.6105	136070.4120	5651807.13
231	0.01356	2.37429	77.108	25.369	591.6105	136662.0225	5631221.371
232	0.01361	2.38790	76.825	25.275	591.6105	137253.6329	5610560.079
233	0.01366	2.40156	76.540	25.181	591.6105	137845.2434	5589822.419
234	0.01371	2.41526	76.253	25.087	591.6105	138436.8539	5569007.535
235	0.01376	2.42902	75.966	24.993	591.6105	139028.4644	5548114.56
236	0.01381	2.44283	75.678	24.898	591.6105	139620.0749	5527142.607
237	0.01386	2.45670	75.389	24.803	591.6105	140211.6854	5506090.774
238	0.01392	2.47062	75.098	24.707	591.6105	140803.2959	5484958.142
239	0.01397	2.48459	74.807	24.611	591.6105	141394.9064	5463743.772
240	0.01403	2.49861	74.514	24.515	591.6105	141986.5168	5442446.709
241	0.01408	2.51270	74.220	24.418	591.6105	142578.1273	5421065.979
242	0.01414	2.52683	73.925	24.321	591.6105	143169.7378	5399600.587
243	0.01419	2.54103	73.629	24.224	591.6105	143761.3483	5378049.519
244	0.01425	2.55528	73.331	24.126	591.6105	144352.9588	5356411.742
245	0.01431	2.56959	73.033	24.028	591.6105	144944.5693	5334686.2
246	0.01437	2.58396	72.733	23.929	591.6105	145536.1798	5312871.816
247	0.01443	2.59838	72.432	23.830	591.6105	146127.7902	5290967.493
248	0.01449	2.61287	72.129	23.731	591.6105	146719.4007	5268972.107
249	0.01455	2.62742	71.826	23.631	591.6105	147311.0112	5246884.514
250	0.01461	2.64203	71.521	23.530	591.6105	147902.6217	5224703.544
251	0.01467	2.65671	71.215	23.430	591.6105	148494.2322	5202428.003
252	0.01474	2.67144	70.907	23.328	591.6105	149085.8427	5180056.67
253	0.01480	2.68624	70.598	23.227	591.6105	149677.4532	5157588.3
254	0.01487	2.70111	70.288	23.125	591.6105	150269.0637	5135021.618
255	0.01493	2.71604	69.976	23.022	591.6105	150860.6741	5112355.323
256	0.01500	2.73104	69.663	22.919	591.6105	151452.2846	5089588.083
257	0.01507	2.74611	69.349	22.816	591.6105	152043.8951	5066718.537
258	0.01513	2.76124	69.033	22.712	591.6105	152635.5056	5043745.295
259	0.01520	2.77645	68.716	22.607	591.6105	153227.1161	5020666.932

260	0.01528	2.79172	68.397	22.503	591.6105	153818.7266	4997481.992
261	0.01535	2.80707	68.077	22.397	591.6105	154410.3371	4974188.984
262	0.01542	2.82249	67.755	22.291	591.6105	155001.9475	4950786.384
263	0.01549	2.83798	67.431	22.185	591.6105	155593.5580	4927272.63
264	0.01557	2.85355	67.106	22.078	591.6105	156185.1685	4903646.122
265	0.01564	2.86919	66.780	21.971	591.6105	156776.7790	4879905.223
266	0.01572	2.88491	66.452	21.863	591.6105	157368.3895	4856048.255
267	0.01580	2.90071	66.122	21.754	591.6105	157960.0000	4832073.498
268	0.01588	2.91658	65.791	21.645	591.6105	158551.6105	4807979.191
269	0.01596	2.93254	65.458	21.536	591.6105	159143.2210	4783763.528
270	0.01604	2.94858	65.123	21.426	591.6105	159734.8314	4759424.654
271	0.01612	2.96470	64.787	21.315	591.6105	160326.4419	4734960.671
272	0.01621	2.98091	64.448	21.204	591.6105	160918.0524	4710369.63
273	0.01629	2.99720	64.108	21.092	591.6105	161509.6629	4685649.528
274	0.01638	3.01358	63.767	20.979	591.6105	162101.2734	4660798.314
275	0.01647	3.03005	63.423	20.866	591.6105	162692.8839	4635813.878
276	0.01656	3.04660	63.077	20.752	591.6105	163284.4944	4610694.054
277	0.01665	3.06325	62.730	20.638	591.6105	163876.1049	4585436.617
278	0.01674	3.07999	62.381	20.523	591.6105	164467.7153	4560039.28
279	0.01683	3.09682	62.029	20.408	591.6105	165059.3258	4534499.693
280	0.01693	3.11376	61.676	20.291	591.6105	165650.9363	4508815.438
281	0.01703	3.13078	61.321	20.174	591.6105	166242.5468	4482984.029
282	0.01713	3.14791	60.963	20.057	591.6105	166834.1573	4457002.906
283	0.01723	3.16514	60.604	19.939	591.6105	167425.7678	4430869.436
284	0.01733	3.18247	60.242	19.820	591.6105	168017.3783	4404580.907
285	0.01744	3.19991	59.878	19.700	591.6105	168608.9887	4378134.525
286	0.01754	3.21745	59.512	19.579	591.6105	169200.5992	4351527.413
287	0.01765	3.23510	59.143	19.458	591.6105	169792.2097	4324756.603
288	0.01776	3.25286	58.773	19.336	591.6105	170383.8202	4297819.036
289	0.01787	3.27074	58.400	19.214	591.6105	170975.4307	4270711.558
290	0.01799	3.28873	58.024	19.090	591.6105	171567.0412	4243430.91
291	0.01811	3.30683	57.646	18.966	591.6105	172158.6517	4215973.731
292	0.01823	3.32506	57.266	18.841	591.6105	172750.2622	4188336.549
293	0.01835	3.34341	56.883	18.715	591.6105	173341.8726	4160515.778
294	0.01847	3.36188	56.498	18.588	591.6105	173933.4831	4132507.707
295	0.01860	3.38048	56.109	18.460	591.6105	174525.0936	4104308.503
296	0.01873	3.39921	55.719	18.331	591.6105	175116.7041	4075914.198
297	0.01886	3.41807	55.325	18.202	591.6105	175708.3146	4047320.686
298	0.01900	3.43706	54.928	18.071	591.6105	176299.9251	4018523.714
299	0.01913	3.45620	54.529	17.940	591.6105	176891.5356	3989518.875
300	0.01928	3.47547	54.127	17.808	591.6105	177483.1460	3960301.602
301	0.01942	3.49489	53.722	17.674	591.6105	178074.7565	3930867.157
302	0.01957	3.51446	53.313	17.540	591.6105	178666.3670	3901210.625
303	0.01972	3.53418	52.902	17.405	591.6105	179257.9775	3871326.9
304	0.01987	3.55405	52.487	17.268	591.6105	179849.5880	3841210.68

305	0.02003	3.57408	52.069	17.131	591.6105	180441.1985	3810856.452
306	0.02019	3.59428	51.647	16.992	591.6105	181032.8090	3780258.482
307	0.02036	3.61464	51.223	16.852	591.6105	181624.4195	3749410.801
308	0.02053	3.63517	50.794	16.711	591.6105	182216.0299	3718307.193
309	0.02070	3.65587	50.362	16.569	591.6105	182807.6404	3686941.182
310	0.02088	3.67676	49.926	16.426	591.6105	183399.2509	3655306.01
311	0.02107	3.69782	49.486	16.281	591.6105	183990.8614	3623394.628
312	0.02126	3.71908	49.043	16.135	591.6105	184582.4719	3591199.669
313	0.02145	3.74053	48.595	15.988	591.6105	185174.0824	3558713.438
314	0.02165	3.76218	48.143	15.839	591.6105	185765.6929	3525927.881
315	0.02186	3.78404	47.687	15.689	591.6105	186357.3034	3492834.568
316	0.02207	3.80610	47.227	15.538	591.6105	186948.9138	3459424.666
317	0.02228	3.82839	46.762	15.385	591.6105	187540.5243	3425688.909
318	0.02251	3.85089	46.292	15.230	591.6105	188132.1348	3391617.573
319	0.02274	3.87363	45.817	15.074	591.6105	188723.7453	3357200.439
320	0.02298	3.89661	45.338	14.916	591.6105	189315.3558	3322426.756
321	0.02322	3.91983	44.853	14.757	591.6105	189906.9663	3287285.21
322	0.02348	3.94331	44.363	14.595	591.6105	190498.5768	3251763.869
323	0.02374	3.96704	43.868	14.433	591.6105	191090.1872	3215850.145
324	0.02401	3.99105	43.367	14.268	591.6105	191681.7977	3179530.74
325	0.02429	4.01534	42.860	14.101	591.6105	192273.4082	3142791.585
326	0.02458	4.03992	42.347	13.932	591.6105	192865.0187	3105617.779
327	0.02488	4.06480	41.828	13.761	591.6105	193456.6292	3067993.518
328	0.02519	4.09000	41.302	13.588	591.6105	194048.2397	3029902.015
329	0.02552	4.11552	40.769	13.413	591.6105	194639.8502	2991325.417
330	0.02586	4.14137	40.230	13.236	591.6105	195231.4607	2952244.7
331	0.02621	4.16758	39.683	13.056	591.6105	195823.0711	2912639.566
332	0.02658	4.19416	39.128	12.873	591.6105	196414.6816	2872488.314
333	0.02696	4.22112	38.565	12.688	591.6105	197006.2921	2831767.706
334	0.02736	4.24847	37.994	12.500	591.6105	197597.9026	2790452.805
335	0.02777	4.27625	37.415	12.309	591.6105	198189.5131	2748516.801
336	0.02821	4.30446	36.826	12.116	591.6105	198781.1236	2705930.803
337	0.02867	4.33313	36.228	11.919	591.6105	199372.7341	2662663.607
338	0.02915	4.36228	35.619	11.719	591.6105	199964.3445	2618681.431
339	0.02966	4.39193	35.000	11.515	591.6105	200555.9550	2573947.602
340	0.03019	4.42213	34.370	11.308	591.6105	201147.5655	2528422.202
341	0.03076	4.45288	33.728	11.097	591.6105	201739.1760	2482061.644
342	0.03135	4.48423	33.074	10.881	591.6105	202330.7865	2434818.191
343	0.03199	4.51622	32.407	10.662	591.6105	202922.3970	2386639.372
344	0.03266	4.54888	31.725	10.438	591.6105	203514.0075	2337467.301
345	0.03338	4.58225	31.028	10.208	591.6105	204105.6180	2287237.864
346	0.03414	4.61639	30.316	9.974	591.6105	204697.2284	2235879.728
347	0.03496	4.65136	29.586	9.734	591.6105	205288.8389	2183313.159
348	0.03585	4.68721	28.838	9.488	591.6105	205880.4494	2129448.562

349	0.03680	4.72401	28.070	9.235	591.6105	206472.0599	2074184.68
350	0.03784	4.76185	27.280	8.975	591.6105	207063.6704	2017406.358
351	0.03897	4.80082	26.467	8.708	591.6105	207655.2809	1958981.706
352	0.04020	4.84102	25.628	8.432	591.6105	208246.8914	1898758.48
353	0.04157	4.88258	24.760	8.146	591.6105	208838.5019	1836559.394
354	0.04308	4.92566	23.861	7.850	591.6105	209430.1123	1772175.927
355	0.04476	4.97042	22.927	7.543	591.6105	210021.7228	1705360.021
356	0.04667	5.01709	21.953	7.223	591.6105	210613.3333	1635812.699
357	0.04883	5.06592	20.934	6.887	591.6105	211204.9438	1563168.068
358	0.05134	5.11726	19.863	6.535	591.6105	211796.5543	1486970.216
359	0.05427	5.17153	18.730	6.162	591.6105	212388.1648	1406638.665
360	0.05777	5.22930	17.525	5.766	591.6105	212979.7753	1321414.582
361	0.06205	5.29135	16.230	5.340	591.6105	213571.3857	1230272.675
362	0.06745	5.35880	14.822	4.876	591.6105	214162.9962	1131767.315
363	0.07457	5.43336	13.266	4.364	591.6105	214754.6067	1023739.936
364	0.08457	5.51793	11.501	3.784	591.6105	215346.2172	902692.545
365	0.10016	5.61808	9.411	3.096	591.6105	215937.8277	762180.1332
366	0.13003	5.74811	6.697	2.203	591.6105	216529.4382	587087.0576
367	0.26976	6.01787	1.067	0.351	591.6105	217121.0487	282982.2419
END				0.000	0.00000		

Appendix D. C++ Codes for Generation of ANSYS command Language

C++ Code for Generation of ANSYS Command Language (Thermal Analysis)

```
#include <stdio.h>
#include <string.h>
#include <conio.h>
#include <math.h>

int main ()
{

FILE *input;
input= fopen("c:\\ANSYS_ProgmCodes.txt","w");
float v=0, u=41.67, a=-6.867, A=0.00775;
float alpha=-20.87, teta=1.0471;
float delta_t=0.0, accum_t=0.0;
float w0=126.66, w1, vi, vj, Q, q;
int i,j=1;

for(i=1;i<368;i++)
{
w1=sqrt((w0*w0)+(2*alpha*teta));
delta_t=(w1-w0)/alpha;
vi= (0.329*w0);
vj= (0.329*w1);
Q= 0.95*((0.5*238.25)*((vi*vi)-(vj*vj)));
q=(Q)/(A*delta_t);

fprintf(input,"!Load Step %d\n\n",i);

fprintf(input,"ASEL,ALL\n");
fprintf(input,"SFA,ALL,1,CONV,50,25\n\n");

fprintf(input,"ASEL,S,AREA,,%d\n",j);
fprintf(input,"CM,FLUX%d,AREA\n",j);
fprintf(input,"ASEL,,AREA,,FLUX%d\n",j);
fprintf(input,"SFA,ALL,1,HFLUX,%f\n\n",q);

accum_t+=delta_t;
fprintf(input,"TIME,%f\n",accum_t);
fprintf(input,"AUTOTS,-1\n");
```

```
fprintf(input,"NSUBST,5,,,1\n");
fprintf(input,"KBC,1\n");
fprintf(input,"OUTRES,BASIC,LAST\n");
fprintf(input, "OUTPR,BASIC\n\n");

fprintf(input,"LSWRITE,%d\n\n",i);

fprintf(input,"ASEL,ALL\n");
fprintf(input,"SFADELE,ALL,1,ALL\n\n\n\n\n\n");

fprintf(input,"!***\n");
printf("%3d %f %f\n",i,q,accum_t);

w0=w1;
if(w0<0) break;
j++;
if(j==7) j=1;
}
printf("\nCOMPLETED!\n\nPress Any Key to Exit.. ");
getch();

}
```

C++ Code for Generation of ANSYS Command Language (Thermal Stress Analysis)

```
#include <stdio.h>
#include <string.h>
#include <conio.h>
#include <math.h>

int main ()
{

FILE *input;
input= fopen("d:\\Structural_thermal_stress.txt","w");
float v=0, u=41.67, a=-6.867, A=0.00775;
float alpha=-20.87, teta=1.0471;
float delta_t=0.0, accum_t=0.0;
float w0=126.66, w1, vi, vj, Q, q;
int i;
```

```
for(i=1;i<368;i++)
{
w1=sqrt((w0*w0)+(2*alpha*teta));
delta_t=(w1-w0)/alpha;
vi= (0.329*w0);
vj= (0.329*w1);
Q= 0.95*((0.5*238.25)*((vi*vi)-(vj*vj)));
q=(Q)/(A*delta_t);

fprintf(input,"!Load Step %d\n\n",i);


accum_t+=delta_t;

fprintf(input,"LDREAD,TEMP,,,%f,,Simulation_27_perforated_vented_model_glue
d,rth\n",accum_t);

fprintf(input,"TIME,%f\n",accum_t);
fprintf(input,"AUTOTS,-1\n");
fprintf(input,"KBC,1\n");
fprintf(input,"OUTRES,BASIC,LAST\n");
fprintf(input, "OUTPR,BASIC\n\n");

fprintf(input,"LSWRITE,%d\n\n",i);


w0=w1;
if(w0<0) break;
}
printf("\nCOMPLETED!\n\nPress Any Key to Exit.. ");
getch();

}
```

Appendix E. Top View Temperature Distribution

Perforated Disc Brake (Top View Temperature Distribution)

(a) Time =.51814s

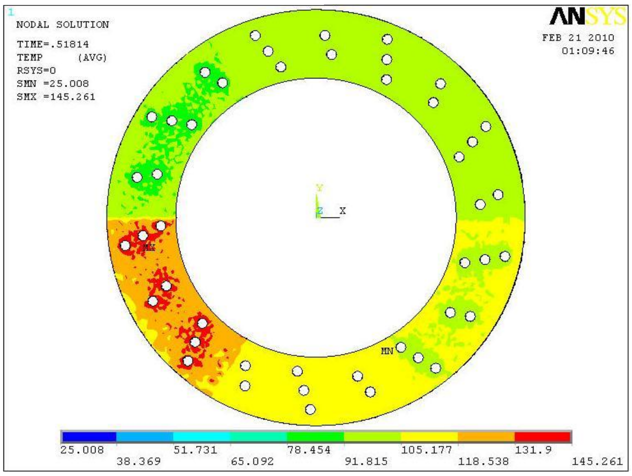

(b) Time =1.09s

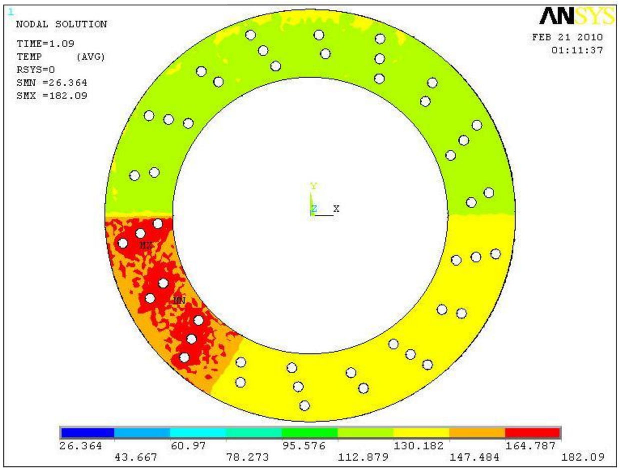

(c) Time =1.736s

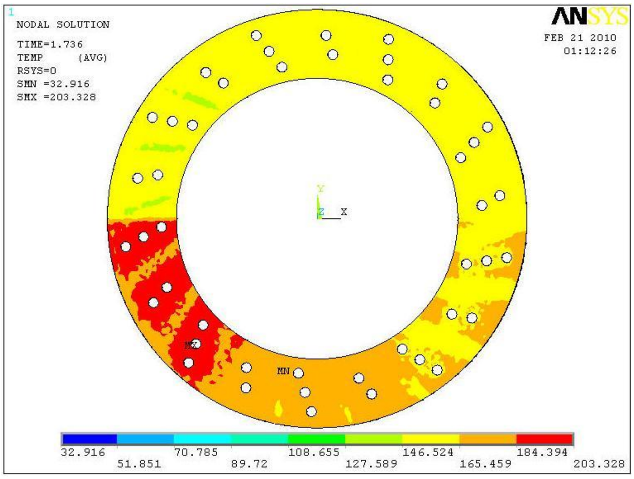

(d) Time =2.498 s

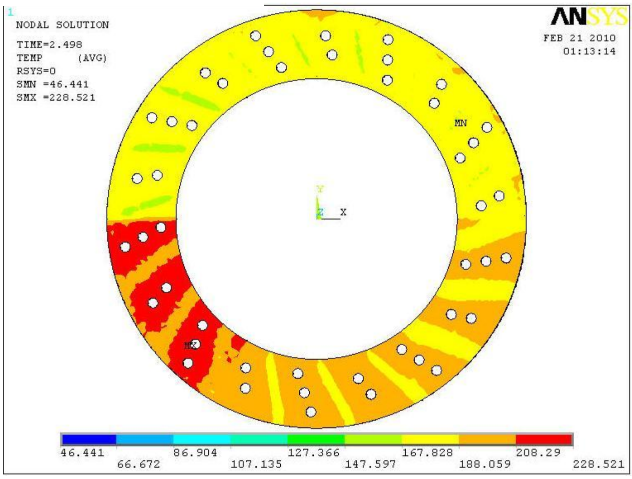

(e) Time =3.475 s

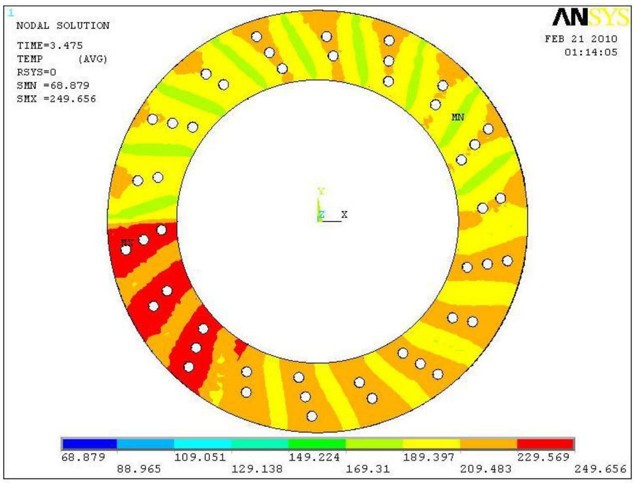

(f) Time =5.99 s

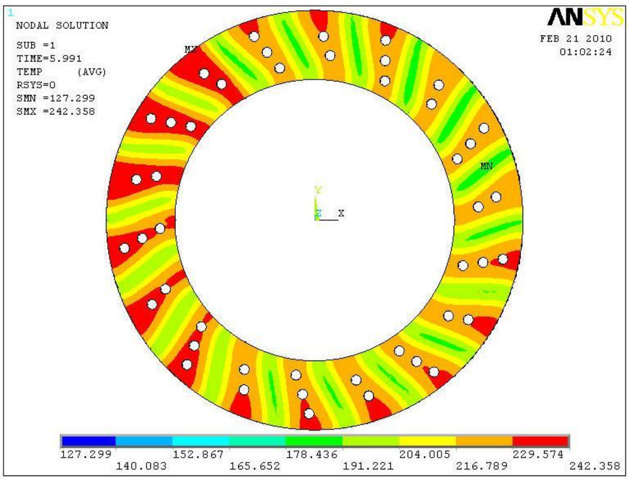

<u>**Non Perforated Disc Brake (Top View Temperature Distribution)**</u>

(a) Time =.51814s

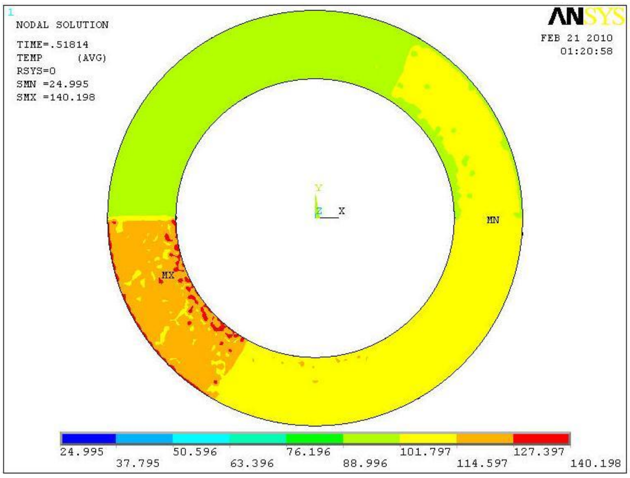

(b) Time =1.09s

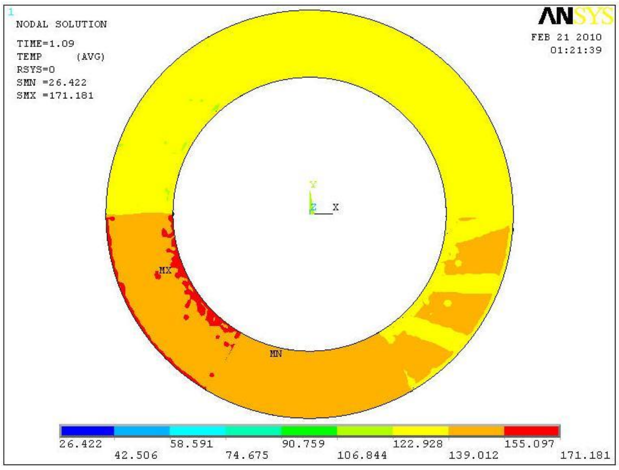

(c) Time =1.736s

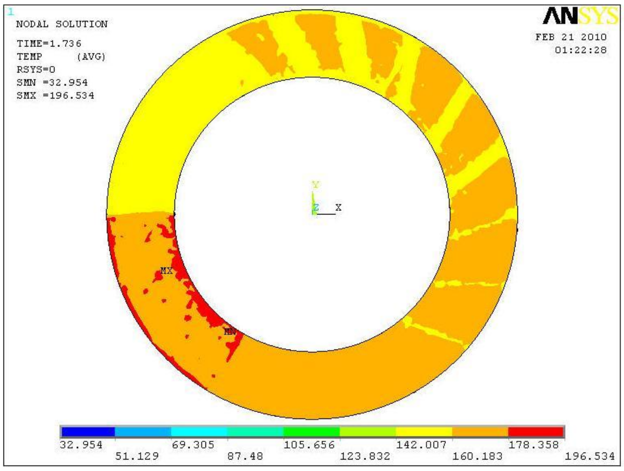

(d) Time =2.498 s

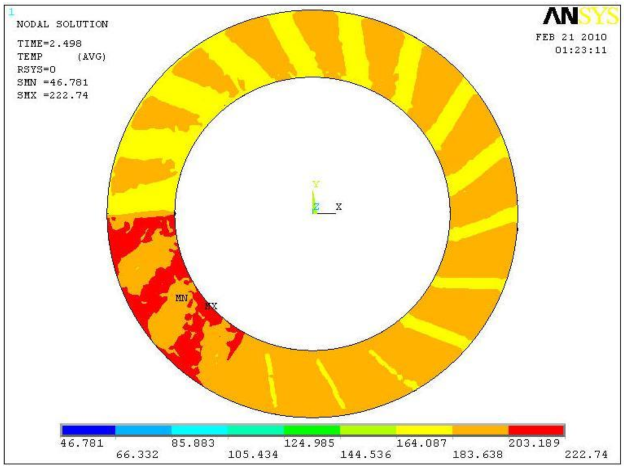

(e) Time =3.475 s

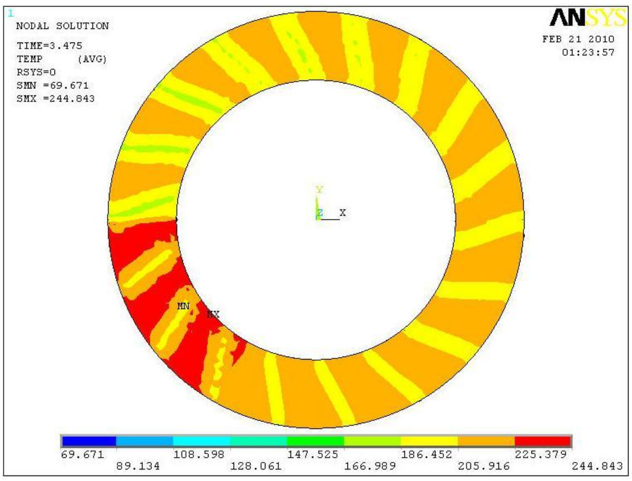

(f) Time =5.99 s

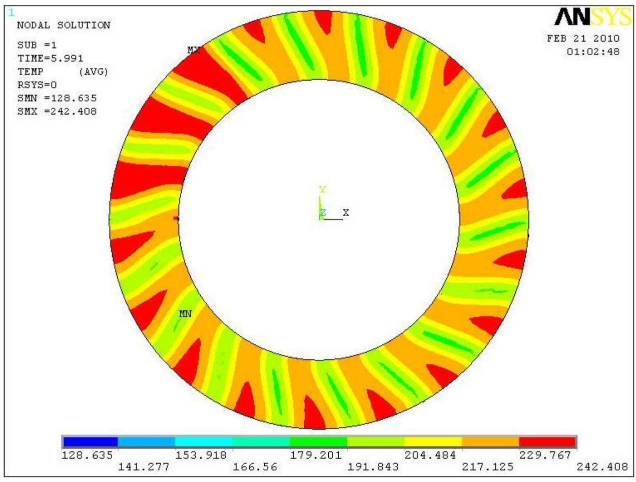

Appendix F. Top View Von Mises Thermal Stress Distribution

Perforated Disc Brake (Top View Von Mises Thermal Stress Distribution)

(a) Time =.51814s

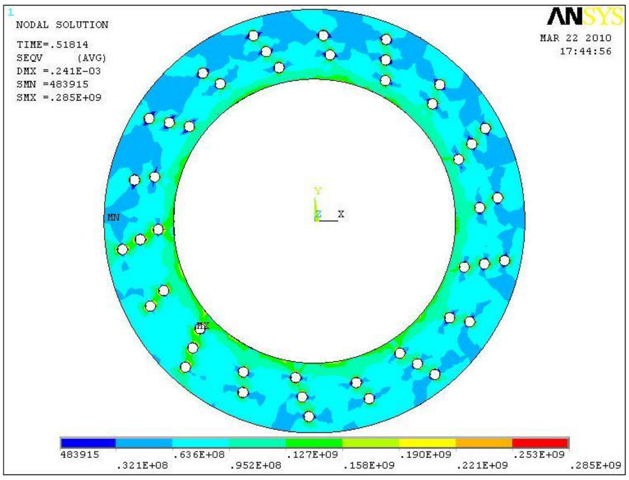

(b) Time =1.09s

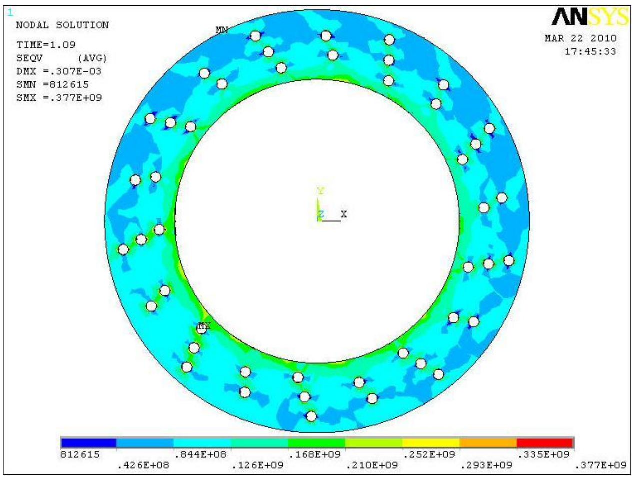

(c) Time =1.736s

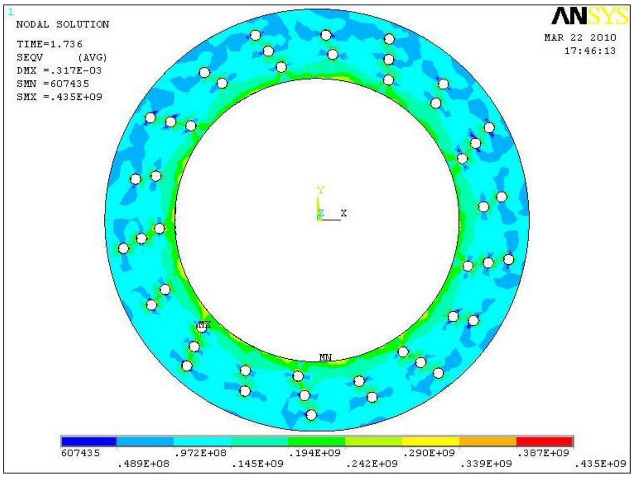

(d) Time =2.498 s

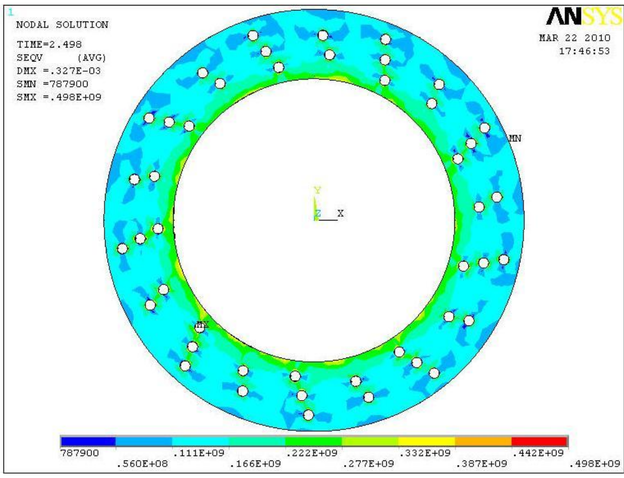

(e) Time =4.2 s

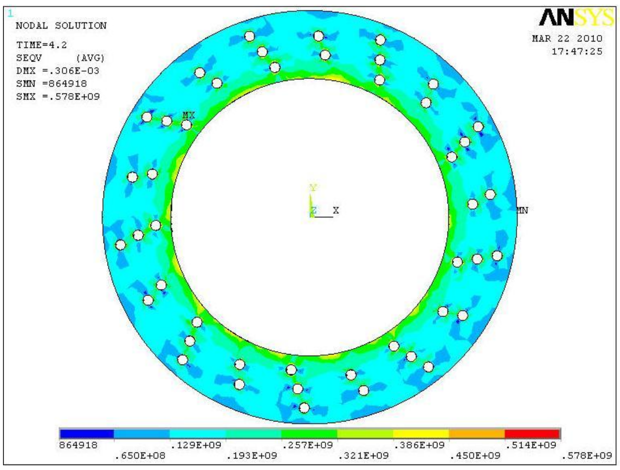

(f) Time =5.99 s

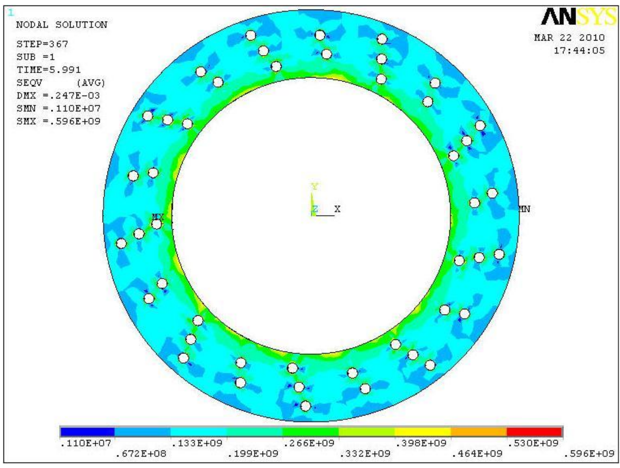

Non Perforated Disc Brake (Top View Von Mises Thermal Stress Distribution)

(a) Time =.51814s

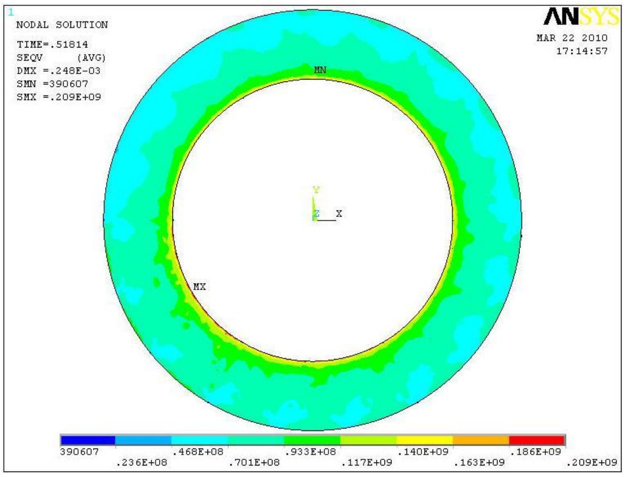

(b) Time =1.09s

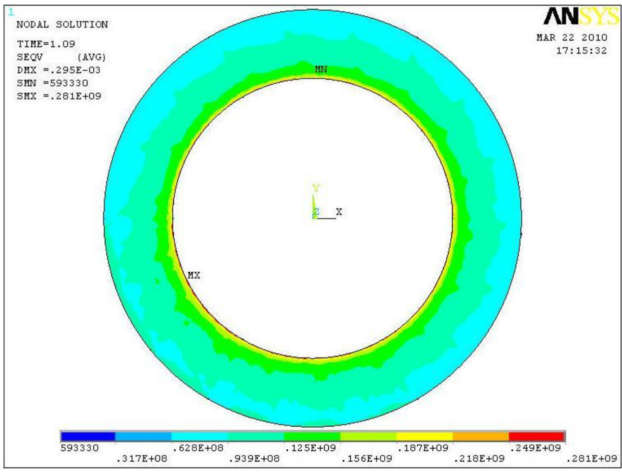

(c) Time =1.736s

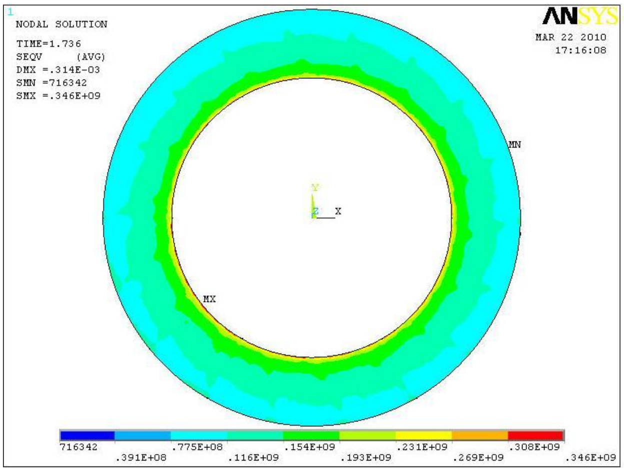

(d) Time =2.498 s

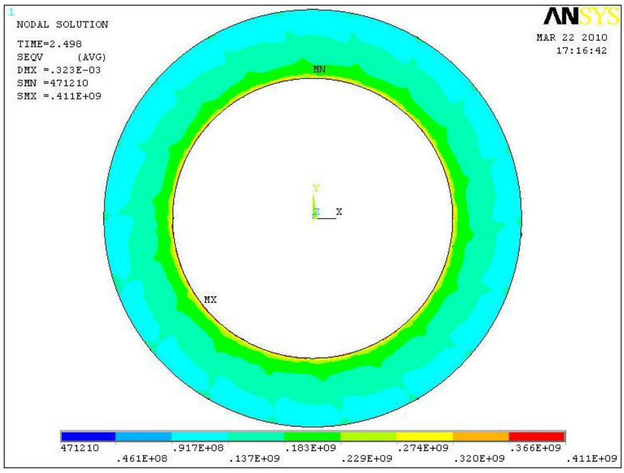

(e) Time =4.2 s

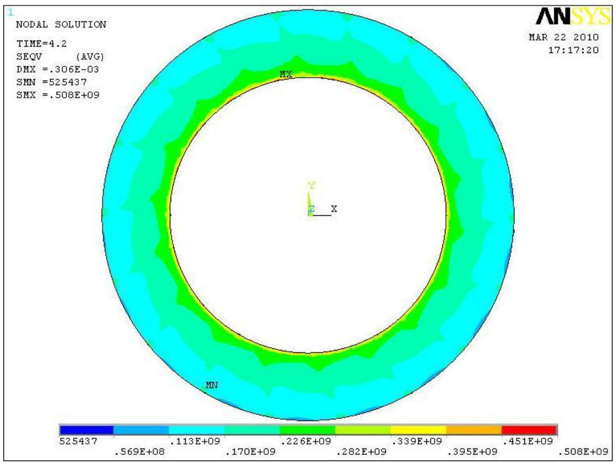

(f) Time =5.99 s

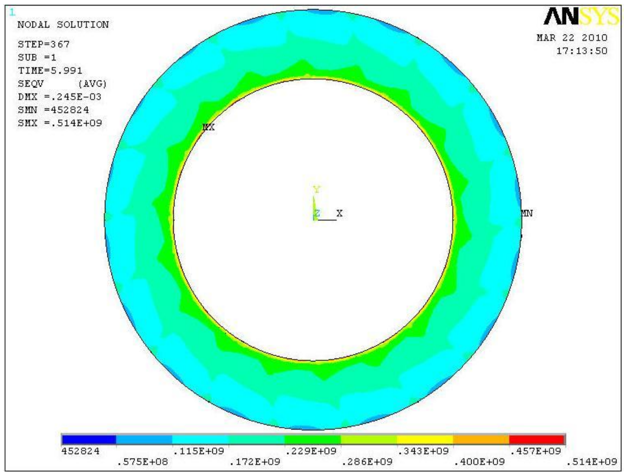

Appendix G. Project Gantt Chart

Final Year Project 1 Gantt Chart

No	Activities / Week	1	2	3	4	5	6	7	8	9	10	11	12	13	14
1	Selection of project topic														
2	Preliminary Research Work														
3	Familiarization of softwares: CATIA and ANSYS														
4	Submission of preliminary report														
5	Data gathering and calculation of initial input (energy)														
6	CAD modeling														
7	Submission of progress report														
8	Seminar														
9	Transferring CAD model to ANSYS and creating C++ command text for ANSYS for analysis work														
10	Simulation on temperature development and distribution														
11	Submission of interim report final draft														
12	Oral presentation														

Final Year Project 2 Gantt Chart

No	Activities / Week	1	2	3	4	5	6	7	8	9	10	11	12	13	14
1	Simulation of thermal stress development and distribution														
2	Submission of progress report 1														
3	Simulation of thermal stress development and distribution continues														
4	Submission of progress report 2														
5	Seminar														
6	Review of project objectives and results														
7	Final report preparation														
8	Poster exhibition														
9	Submission of dissertation final draft														
10	Oral presentation														
11	Submission of dissertation (hard bound)														